

SECOND QUARTERLY REPORT

DEVELOPMENT OF HIGH-PERFORMANCE LIGHT-WEIGHT ELECTRODES

FOR HYDROGEN-OXYGEN FUEL CELLS

by

D. Gershberg, Principal Investigator

W. P. Colman

J. DiPalma

prepared for

NATIONAL AERONAUTICS AND SPACE ADMINISTRATION

January 27, 1966

CONTRACT NAS 3-6477

Period Covered: July 6, 1965 - October 5, 1965

NASA Lewis Research Center
Cleveland, Ohio
Space Power Systems Division
Technical Manager: Mr. Meyer R. Unger

AMERICAN CYANAMID COMPANY
STAMFORD RESEARCH LABORATORIES
1937 West Main Street
Stamford, Connecticut 06904
(Area Code 203) 348-7331

TABLE OF CONTENTS

	<u>PAGE</u>
1. <u>INTRODUCTION</u>	1
1.1 Objectives	1
1.2 Scope	2
2. <u>SUMMARY</u>	3
3. <u>SMALL CELL TESTING</u>	7
3.1 Investigation of Matrix Materials	7
3.1.1 Magnesia	7
3.1.2 Ceria-PTFE	7
3.1.3 Thoria-PTFE	10
3.2 Investigation of Operating Variables	13
3.2.1 Pressure	16
3.2.2 Temperature	19
3.2.3 KOH Concentration	21
3.2.4 Regions of Unstable Operation	23
3.2.5 Highest Performance Levels	23
3.3 Life-Testing	31
3.3.1 Tests at 100°C	31
3.3.2 Tests at 125°C	34
3.3.3 Tests at 150°C	37
3.3.4 Polarization Data on Used Electrodes	38

TABLE OF CONTENTS

(Continued)

	<u>PAGE</u>
4. <u>LARGE CELL FABRICATION</u>	41
5. <u>LARGE CELL TESTING</u>	44
5.1 Initial Performance	44
5.2 Life Tests	44
6. <u>FUTURE WORK</u>	51
7. <u>REFERENCES</u>	52

LIST OF TABLES

<u>TABLE</u>	<u>TITLE</u>	<u>PAGE</u>
3-1	Performance of Ceria-PTFE Matrices	8
3-2	Performance of Thoria-PTFE Matrix	12
3-3	Optimum KOH Loading	14
3-4	Investigation of Operating Variables	17
3-5	Life Tests: 2" x 2" Cells:	28
5-1	Initial Performance: 6" x 6" Cell	45
5-2	Life Tests: 6" x 6" Cell	47

LIST OF FIGURES

<u>FIGURE</u>	<u>TITLE</u>	<u>PAGE</u>
3-1	KOH Corrosion of Ceria-PTFE Matrix at 150-200°C	9
3-2	Average Voltage Changes During Successive Polarization Curves	15
3-3	Effect of Pressure on Performance	18
3-4	Effect of Temperature on Performance	20
3-5	Effect of KOH Concentration on Performance	22
3-6	Life Tests at 100°C: ACCO-I Asbestos Matrix	24
3-7	Life Tests at 100°C: ACCO-II Asbestos Matrix	25
3-8	Life Tests at 125°C: Asbestos Matrices	26
3-9	Life Tests at 125-150°C: Experimental Matrices	27
3-10	Polarization Data on Used Electrodes	39
4-1	6" x 6" Cell: Flat Plate Design	42
4-2	6" x 6" Cell: Land and Groove Design	43
5-1	Life Test, 6" x 6" Cell	48

1. INTRODUCTION

1.1 Objectives

Light-weight fuel cell batteries capable of producing large quantities of energy appear feasible for space applications. High-performance light-weight electrode systems are an essential part of these batteries. Work completed previously⁽¹⁾, under NASA Contract NAS 3-2786, showed that American Cyanamid AB-40 electrodes (40 mg Pt/cm²) give high and sustained performance in hydrogen-oxygen matrix fuel cells including those of battery size; this performance is substantially higher than that of American Cyanamid AB-1 electrodes which contain less platinum (9 mg Pt/cm²). It was calculated that at temperatures up to 100°C, the AB-40 electrodes could be incorporated in a 2 kw fuel battery whose weight per net power (including all auxiliaries except fuel and tankage) would be approximately 50 lb/kw.

A detailed investigation at temperatures up to 100°C showed that initial performance generally increases with increasing temperature, pressure, and electrolyte (KOH) concentration. Furthermore, preliminary studies demonstrated that substantial increases in initial performance can be obtained by operating at higher temperatures (140°C) and KOH concentrations (65%), than are generally employed in matrix fuel cells. Under these conditions current densities as high as 100, 400 and 800 ma/cm² at working voltages of 1.0, 0.9 and 0.8 v, respectively, were achieved in short term tests.

Accordingly the objective of the present contract is to investigate and recommend preferred conditions, at 100-200°, under which AB-40 electrodes would be capable of sustained high performance in a total module having a weight-to-power ratio substantially lower than those presently available for space environment.

1.2 Scope

The scope of work to be done by American Cyanamid Company during the Contract year is outlined in the Schedule of Work presented in the First Quarterly Report.

Work in the second quarter of the contract was devoted to Tasks I-A, I-B, II and III. In Task I-A, an experimental investigation of the effects of pressure, temperature, and KOH concentration on initial performance was completed. The development of an empirical model relating initial performance to these variables was begun. The evaluation of novel experimental matrices for use at temperatures up to 150-200°C was continued. In Task II-A small cell life tests were conducted with asbestos matrices and with several novel types of experimental matrices. Six inch by six inch cells were designed for large cell testing at pressures up to 60 psig and fabrication was scheduled, (Task II). Initial performance scale-up studies and large cell life testing were conducted in a 6 inch x 6 inch cell previously available (Task III).

2. SUMMARY

Task I-A

1. The use of PTFE-bonded ceramic powders as matrix materials at 100-200°C is under investigation.

a. Magnesia is unsuitable at 200°C since it dissolves completely in excess 70% KOH within 500 hours.

b. Ceria has good corrosion resistance at 150°C but not at 200°C. An experimental ceria-PTFE matrix (14% PTFE by weight) gave slightly lower performance than Fuel Cell Asbestos at 100°C. At 200°C this matrix permitted electrode-electrode contact similar to that encountered previously⁽²⁾ with PTFE matrices. Matrices with lower PTFE levels are to be investigated.

c. An experimental thoria-PTFE matrix obtained from Chemcell Incorporated gave performance at 150°C equal to that of Fuel Cell Asbestos. Further work in this area will be directed toward improving the bubble pressure and determining the corrosion resistance of thoria at 150-200°C.

2. The investigation of the effects of temperature (100-150°C), pressure (0-60 psig), and KOH concentration (30-75%) on initial performance was completed. The highest working voltages obtained at current densities of 100, 400 and 1000 ma/cm² were 1.10 v, 0.95 v, and 0.82 v, respectively. An empirical model is being developed to give close estimates of initial performance at any point in the operating region defined above. The following tentative conclusions may be drawn from an inspection of the raw data.

a. Performance rises substantially with increasing pressure at all current densities, the magnitude of the improvement increasing with increasing current density. Direct determinations show that a pressure

increase from 0 psig to 60 psig increases voltage by 50-80 mv at 100 ma/cm² 110-120 mv at 400 ma/cm² and 160-350 mv at 1000 ma/cm².

b. Increasing temperature, in the range 100-150°C, improves performance only at KOH concentrations close to the solubility limit. Under these conditions, the improvement becomes more pronounced at high current densities.

c. The effect of KOH concentration on performance depends on the current density and on temperature. At low current densities, performance increases as the concentration is increased to within 5% of the solubility limit. At high current densities, maximum performance is reached at concentrations ranging from 5-25% below the solubility limit.

Task I-B

1. Available matrices were life-tested to determine suitable ranges of temperature, pressure, KOH concentration and current density for long term performance. The matrices included one or more types of asbestos, PTFE, PTFE-Asbestos and PTFE-zirconia. The maximum levels of the operating variables investigated were 150°C, 15 psig, 70% KOH and 400 ma/cm².
2. ACCO-I Asbestos gives stable long-term performance at 100°C, but was found to be borderline at 125°C and unsuitable at 150°C because of corrosion and apparent occlusion of asbestos in the electrode pores. At 100°C, stable operation (≤ 4 mv loss/100 hrs) has been achieved at current densities up to 300 ma/cm² but not yet at 400 ma/cm². At 400 ma/cm², as at lower current densities, pre-wetting the electrodes prior to cell assembly improves the voltage stability.

3. ACCO-II Asbestos appears to be suitable for long term performance at 100°C but not at 125°C. Very stable performance (0.6 mv decline/100 hrs.) was achieved at 100°C, 50% KOH and 0 psig for 1200 hours at 100 ma/cm². The final voltage was 0.931. Stable performance has not yet been achieved at higher current densities.
4. Life tests at pressures up to 15 psig were run with the ACCO-II Asbestos matrix at 100°C and 50% KOH. Stable performance for 120 hours at 100 ma/cm² was demonstrated. Maximum voltage at 15 psig was 0.97 v.
5. A PTFE-Asbestos matrix gave stable performance at 125°C and 100 ma/cm² for 500 hours, but then failed abruptly due to cross-leakage of gas. Performance at 300 ma/cm² was very unstable. Rapid performance declines were also observed in tests at 150°C.
6. Commercial PTFE felt, zirconia paper, and Zirconia-PTFE sheet gave very high voltage decline rates at 100°C because of severe gas cross-leakage.
7. Commercial PTFE sheets less than 20 mils thick permitted electrode-electrode contact. A 20 mil thick etched PTFE matrix gave stable performance at 125°C and 100 ma/cm² for 540 hours but at a relatively high resistance and low voltage (0.90-0.92 v). After 540 hours, the voltage declined abruptly because of gas cross-leakage which in turn appears to have resulted from a loss in wettability of the etched surface.

Task II

A 6" x 6" active area cell was designed for large cell life-testing at pressures up to 60 psig. The gas distribution system is the same as that of the flat plate 6" x 6" cell currently in use. Lands and grooves together with an "O" ring provide a gas and liquid seal. In this respect the cell is similar to the 2" x 2" pressure cell. Fabrication was scheduled for three cells of this design.

Task III

Tests in a flat plate 6" x 6" cell, designed previously, showed that a 45-fold scale-up in electrode area caused no change in initial performance at current densities up to at least 600 ma/cm².

Life tests were conducted in the 6" x 6" cell at 100°C and atmospheric pressure. The removal of product water simulated that of a battery system operating with a recycle hydrogen stream and dead-ended oxygen. Stable performance was obtained at 100-200 ma/cm² for 100-200 hours but not yet at higher current densities. At 300 ma/cm², voltage stability appears to increase with increasing humidity of the inlet hydrogen stream. It appears that the electrodes can withstand high rates of hydrogen impingement (2500-3500 cc/min) for a prolonged period (800 hours) without being seriously eroded.

3. SMALL CELL TESTING

3.1 Investigation of Matrix Materials

An evaluation was begun of matrix materials made from magnesia, ceria, or thoria, bonded with PTFE. Screening procedures included beaker corrosion testing of the powder or matrix, initial performance determinations, and bubble pressure measurements.

3.1.1 Magnesia

Magnesia powder dissolved completely in 75% KOH at 200°C within 500 hours and so is not suitable at this temperature.

3.1.2 Ceria-PTFE

Proprietary ceria-PTFE matrices containing 75% and 86% ceria by weight were evaluated. These matrices are 9 mils thick, and have 72-77% total voids.

An 86/14 ceria-PTFE matrix was corrosion-tested at 150°C in 70% KOH, and at 200°C in 75% KOH. In both tests the matrix pores were completely filled with electrolyte. Results are shown in Figure 3-1. At 200°C, 27% of the matrix dissolved after 380 hours. However, at 150°C only 4% of the matrix dissolved after 900 hours. Since PTFE does not dissolve under these conditions, all of the dissolved material was ceria. Thus, the matrix appears promising for use at 150°C but not at 200°C unless the corrosion rate in the cell, where there is no large excess of electrolyte, is considerably less than shown by the beaker corrosion test.

The initial performance of ceria-PTFE matrices at 100°-200°C is shown in Table 3-1. The matrices were loaded with 50% KOH by immersion for 24 hours. The 86/14 ceria-PTFE matrix held more 50% KOH (1.5 cc/cm³)* than the 75/25 matrix (1.0 cc/cm³). At 100°C the resistance of the 86/14 matrix (0.045 ohm) was slightly above that of 20 mil Fuel Cell Asbestos (0.038 ohm). Its performance was 10-20 mv below that of the asbestos matrix

*cm³ of dry matrix- a loading greater than the void fraction of the dry matrix indicates that the matrix swells in KOH.

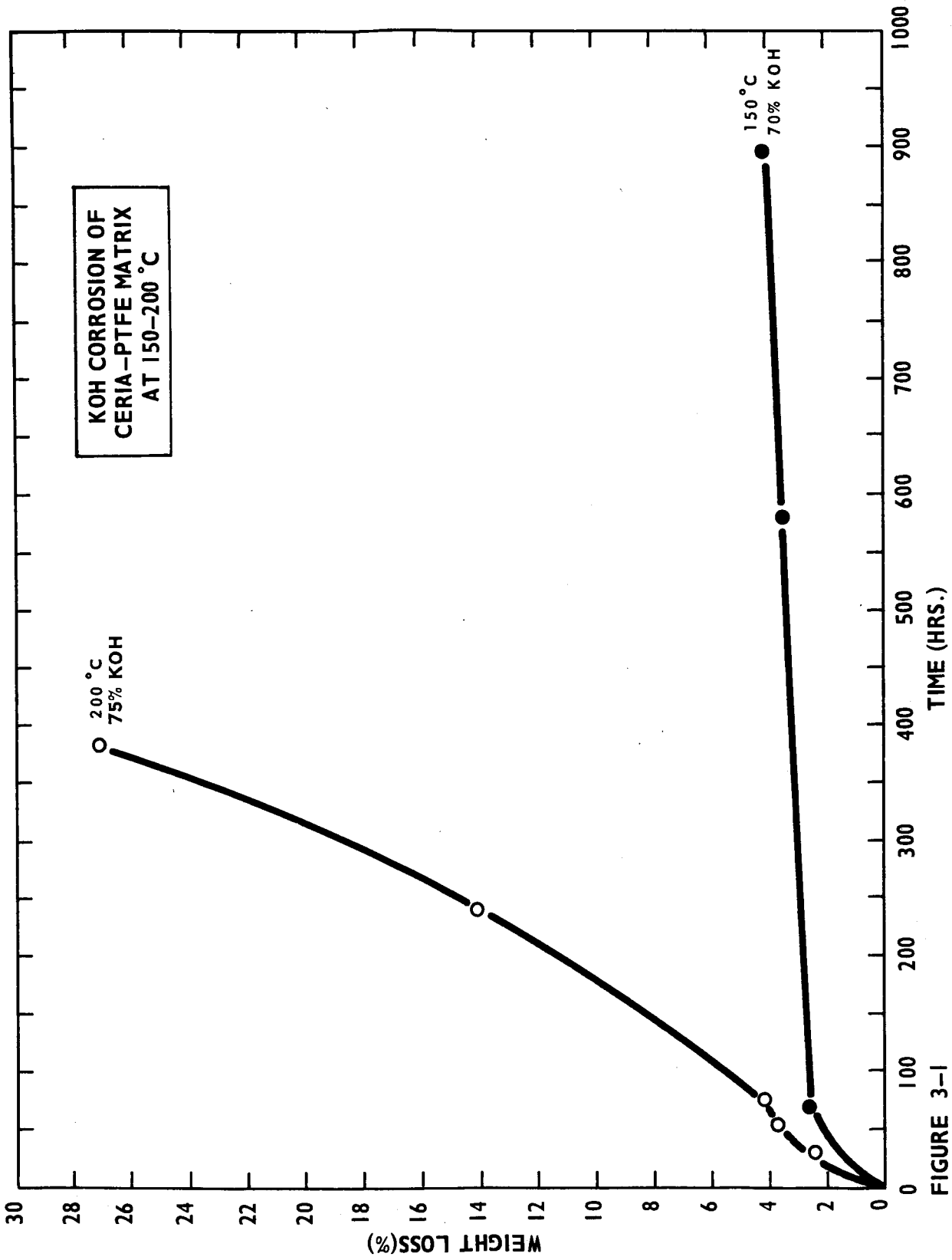


FIGURE 3-1

TABLE 3-1

Performance of Ceria-PTFE Matrices

Cell: 1"
Electrodes: AB-40
Pressure: 0 psig

Weight Ratio Ceria/PTFE in Matrix	Matrix Thickness (Mils)	Temp. (°C)	KOH Conc. (Wt. %)	KOH Loading cc KOH cm ³ Dry Matrix	Cell Assembly Pressure (psi)	Cell Resistance (Ohms)	Working Voltage at Current Density (ma/cm ²) of							
							0	100	200	300	400	500	600	800
86/14	9	100	50	1.5	180	.045	1.07	.96	.90	.84	.79	.66	.51	.32
		200	75	0.9	180	.020	.02(b)	-	-	-	-	-	-	-
		100	50	0.9	180	.018	.005(b)	-	-	-	-	-	-	-
86/14	9	200	50-	1.5-	60	.044	1.07(c)	.98	.94	.89	.82	.68	↑	↓
			75	0.9										
75/25	9	200	75	0.6	180	.018	0(b)	-	-	-	-	-	-	-
75/25	18(a)	200	75	0.6	180	.25	1.10	.1	-	-	-	-	-	-

(a) 2 sheets

(b) Electrodes broke through matrix

(c) First polarization

↑ Unstable

at current densities up to 600 ma/cm² and was much lower than that of asbestos at higher current densities. Following the run at 100°C, the cell was heated to 200°C. However, no performance was obtained at 200°C or, after cooling, at 100°C. Since a few pinholes were found in the matrix, it appears that the total loss of performance was caused either by gas leakage or by electrode-electrode contact. Electrode breakthrough was avoided in a second run at 200°C by tightening the cell to only 60 psi instead of the usual 180 psi. The resistance was 0.044 ohm and a first polarization curve was obtained at current densities up to 600 ma/cm². However, while attempting to run a second polarization curve, the resistance rose suddenly to 0.16 ohm and no performance was obtained. The reason for this is not clear. With one sheet of the 75/25 ceria-PTFE matrix, electrode breakthrough occurred at 200°C in a cell tightened to 180 psi. Two sheets of this matrix produced very high cell resistance probably because of the low loading (0.6 cc/cm³) of 75% KOH.

The performance of the ceria-PTFE matrix appears to improve with decreasing PTFE content. The 86/14 matrix contains 35% PTFE by volume. Matrices containing 25% and 15% PTFE by volume will be evaluated.

3.1.3 Thoria-PTFE

Thoria is reported to have high corrosion resistance to molten KOH at 400°C, ⁽³⁾ higher than that of any other ceramic oxide tested. While this does not necessarily mean that thoria will have high corrosion resistance in aqueous KOH at 150-200°C, the material warrants investigation. The radioactivity of thoria does not necessarily bar its use as a matrix material.

An experimental thoria-PTFE matrix was obtained from Chemcell Inc. This matrix contains 70% thoria by weight, is 20 mils thick and has 72-74% voids.

It absorbed 0.4 cc KOH/cm³ after 24 hours immersion in the electrolyte. Much higher loadings (0.9-1.0 cc/cm³) were obtained by immersing the matrix in KOH and then alternately pulling and releasing vacuum for five minutes. Longer periods did not further increase the loading. Since these loadings are greater than the maximum indicated by the void volume, the matrix must swell slightly in KOH.

Initial performance was obtained in duplicate runs at 100°C, 150°C and 200°C. The KOH concentrations at these respective temperatures were 50%, 68% and 75%. At 100°C, the KOH concentration was 50% and the maximum loading of 1.0 cc/cm³ was used. Since higher KOH concentrations were reached by concentrating in the cell, the loadings at these concentrations were correspondingly lower. Results are shown in Table 3-2. Although the voltage levels in the duplicate runs were not in close agreement, both runs yielded performance at 100°C and 200°C substantially below that of asbestos-containing matrices having the same resistance. Thus at 100°C, the voltage was at least 40 mv and 120 mv below that reported previously for 20 mil Fuel Cell Asbestos⁽²⁾ at 100 and 400 ma/cm², respectively and was unstable at current densities above 200-400 ma/cm². At 200°C the voltage was at least 110 mv and 140 mv below that reported previously⁽²⁾ for 75/25 PTFE-asbestos at 100 and 400 ma/cm², respectively. By contrast at 150°C, the better of the two runs yielded performance equal to that of ACCO-II Asbestos (Section 3.2). Working voltages of 1.01 v and 0.86 v were obtained at 100 and 400 ma/cm², respectively.

The variability in performance observed with this matrix may have been due to the different final KOH loadings used at the different temperatures. Cross-leakage of gases is another possible source of difficulty, since this matrix has a very low bubble pressure (less than 4 inches of water).

TABLE 3-2

Performance of Thoria-PIFE Matrix (1)

Cell: 1"
Electrodes: AB-40
Pressure: 0 psig

Temp. (°C)	KOH Conc. (%)	KOH Loading (cc KOH/cm ³ Dry Matrix)	Cell Resistance (Ohms)	Working Voltage at Current Density (ma/cm ²) of:										
				0	100	200	300	400	600	800	1000			
100	50	1.0	.052	1.16	.89	.77	↑	↓	.80	.63	.46	↓	↓	.33
150	68	0.7	.045	-	1.01	.94	.87	.80	.68	.46	↓	↓	↓	-
200	75	0.6	.060	1.07	.95	.87	.78	.68	.46	↓	↓	↓	↓	-
100	50	1.0	.038	1.15	.92	.82	.71	.53	↓	.71	.59	↓	↓	-
150	68	0.7	.037	-	1.02	.97	.92	.86	.79	.71	.59	↓	↓	-
200	75	0.6	.040	1.07	.97	.92	.86	.79	.59	.59	.59	↓	↓	-

(1) Chemcell, Inc.; 70% Thoria, 30% PIFE by weight

3.2 Investigation of Operating Variables

The investigation of the effects of temperature (100-150°C), pressure (0-60 psig), and KOH concentration (30-75%) on initial performance at 0-1000 ma/cm² was completed. The matrix was ACCO-II Asbestos, 16-18 mils thick. All runs included in the experimental design⁽²⁾ were made, together with five additional runs.

The optimum KOH loading used in this investigation was determined at or near the ends of the temperature-concentration range, i.e., at 100°C - 45% KOH and 150°C - 75% KOH. At both temperature-concentration levels, the optimum loading was 1.0 cc KOH/cm³ dry matrix (Table 3-3). This is also the maximum KOH loading possible with this matrix at 75% KOH, obtained by concentrating 50% KOH within the cell.

In nearly all runs three successive polarization curves were determined. Figure 3-2 shows the average change in voltage between successive curves (1 → 2, and 2 → 3) as a function of current density. The voltage changes were averaged separately for those runs in which the electrolyte was concentrated in the cell during the first polarization curve (all runs at concentrations greater than 50%), and those runs in which it was not.

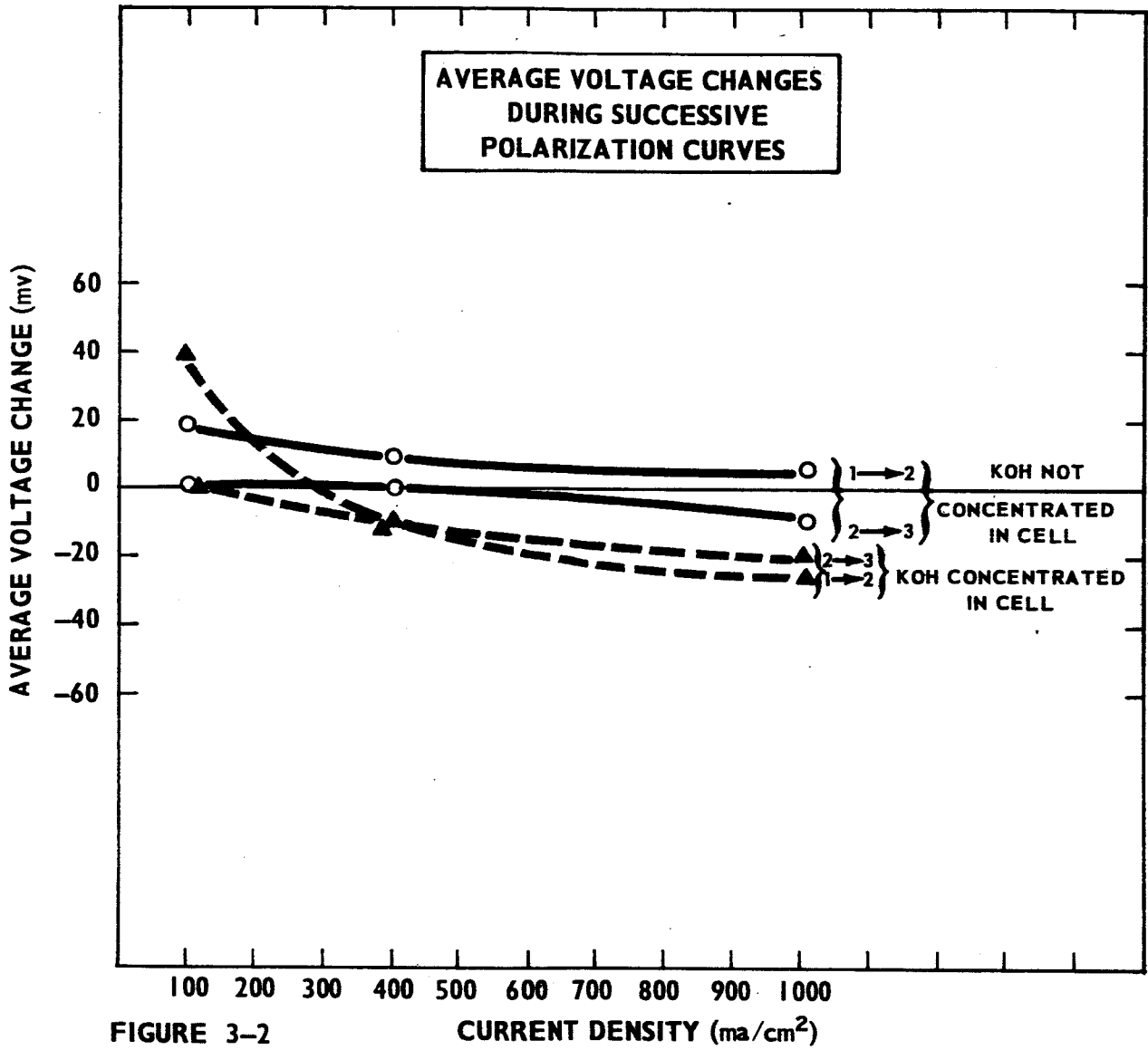
When the electrolyte was not concentrated in the cell, the voltage increased from the first to the second polarization by an average of 20 mv at 100 ma/cm², 10 mv at 400 ma/cm², and 3 mv at 1000 ma/cm². Insignificant voltage changes occurred between the second and third polarization curves. These results agree with those reported previously⁽¹⁾. When the electrolyte

TABLE 3-3

Optimum KOH Loading

Cell: 1"	Electrodes: AB-40	Matrix: 16 mil ACCO-II Asbestos	Pressure: 0 psig	KOH Conc. (wt. %)	Pressure (psig)	KOH Loading cc KOH / cm ³ Matrix	Cells Resistance (Ohms)	Working Voltage at Current Density (ma/cm ²) of:									
								0	50	100	200	300	400	600	800	1000	
100				45	0	.60	.027	1.06	.93	.83	↓	.89	.85	.82	.76	.69	.62
"				"	"	.84	.029	1.06	.96	.93		.89	.85	.81	.74	.67	.58
"				"	"	1.0	.028	1.06	.96	.93		.89	.85	.81	.74	.67	.58
"				"	"	1.2	.025	1.06	-	.91		.83	.75	.68	↓	-	-
150				75	0	.47	.135	1.15	1.05	1.00	-	-	.84	↓	-	-	-
"				"	"	.66	.067	1.16	1.08	1.03	.95	.78	.86	.79	.59	.43	↓
"				"	"	1.0	.063	1.17	1.08	1.04	.96	.79	.87	.79	.61	-	↓

↓ Unstable



was concentrated in the cell, the average voltage increased from the first to the second polarization by 40 mv at 100 ma/cm², 0 mv at 300 ma/cm², and then decreased at higher current densities, reaching a loss of 26 mv at 1000 ma/cm². The third polarization voltages were the same as those of the second polarization at current densities up to 200-400 ma/cm², but at higher current densities the average voltage declined still further by as much as 20 mv. The latter decline reflects the general difficulty of maintaining steady performance for even short periods at high current densities as the KOH concentration approaches the solubility limit. (See Section 3.2.4).

For all runs, the second polarization curve was assumed to be representative and was used to determine the effects of operating variables on performance. Table 3-4 lists second polarization values rounded off to the nearest 10 mv. Based on these data, work was begun on an empirical model which can closely estimate the initial voltage at any point within the region investigated. Effects of the variables which can be determined directly from the data are discussed in the following sections.

3.2.1 Pressure

The effect of pressure on performance over the entire range of temperature and concentration studied is shown in Figure 3-3. Voltages are given for current densities of 100, 400, and 1000 ma/cm². Increased pressure increased the performance substantially at all levels of the

TABLE 3-4

Investigation of Operating Variables

Cell: 1"
 Electrodes: AB-40
 Matrix: ACCO-II Asbestos (16-18 mils)
 KOH Loading: 0.9-1.0 cc/cm² Dry Matrix

Temp. (°C)	KOH Conc. (%)	Pressure (Pslg)	Cell Resistance (Ohms)	Working Voltage at Current Density (ma/cm ²) of:								
				0	50	100	200	300	400	600	800	1000
100	30	0	.043	1.06	.95	.91	.86	.81	.78	.70	.62	.52
"	"	60	.022	1.10	1.01	.99	.95	.92	.90	.87	.83	.81
"	45	0	.028	1.06	.96	.93	.89	.85	.81	.74	.67	.58
"	"	15	.022	1.07	.99	.97	.93	.90	.87	.82	.78	.74
"	"	30	.023	1.09	1.01	.98	.95	.92	.89	.85	.81	.77
"	60	0	.037	1.09	1.01	.98	.92	.86	↓	-	-	-
"	"	30	.025	1.10	1.04	1.01	.96	.91	.87	.77	↓	↓
"	"	60	.057	1.15	1.06	1.03	.98	.94	.89	.80	.72	↓
125	30	15	.023	1.05	.98	.95	.90	.86	.84	.80	.75	↓
"	"	30	.020	1.08	.99	.96	.92	.90	.87	.83	.80	.77
"	45	15	.032	1.08	1.00	.97	.93	.89	.86	.80	.75	.70
"	"	"	.031	1.06	.99	.97	.93	.89	.86	.81	.76	.71
"	"	"	.029	1.06	.99	.97	.93	.89	.86	.80	.75	.69
"	"	"	.023	1.08	1.01	.98	.94	.90	.87	.81	.75	.70
"	"	30	.018	1.08	1.01	.99	.96	.92	.90	.85	.81	.78
"	60	15	.024	1.10	1.04	1.01	.98	.94	.91	.85	.77	.68
"	"	30	.027	1.13	1.06	1.03	.98	.94	.91	.84	.75	.66
"	65	30	.025	1.14	1.07	1.04	1.00	.96	.93	.86	↓	-
150	30	60	.028	1.06	1.00	.97	.92	.88	.84	↓	-	-
"	45	30	.020	1.08	1.03	1.00	.97	.94	.90	.86	.81	.77
"	"	60	.022	1.10	1.06	1.03	1.00	.97	.94	.90	↓	-
"	55	0	.026	1.08	1.02	.99	.93	.88	.84	.74	.62	.47
"	"	30	.024	1.12	1.05	1.02	.98	.95	.92	.87	.82	.77
"	"	60	.021	1.13	1.07	1.05	1.01	.98	.95	.90	.86	.82
"	60	30	.024	1.10	1.05	1.02	.99	.95	.92	.85	.79	.73
"	65	0	.037	1.12	1.04	1.01	.95	.90	.86	.75	.63	.52
"	"	15	.025	1.12	1.06	1.03	.99	.95	.91	.84	.76	.66
"	75	0	.050	1.15	1.10	1.05	.98	.92	.86	.71	.58	.48
"	"	30	.045	1.19	1.12	1.08	1.03	.98	.93	.84	.75	.69
"	"	60	.064	1.21	1.13	1.10	1.03	.98	.92	.81	.71	.64

↓ Unstable performance

EFFECT OF PRESSURE ON PERFORMANCE

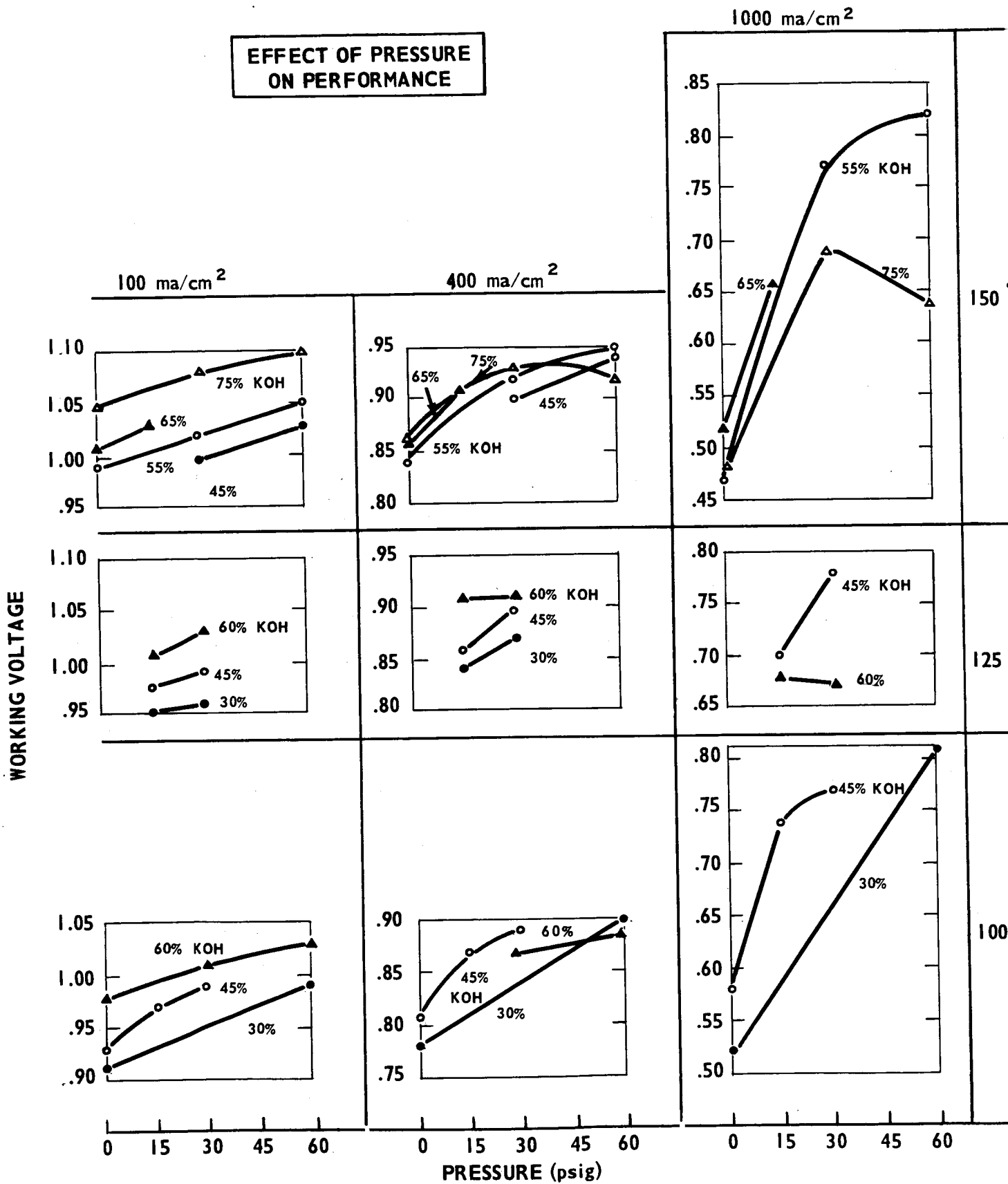


FIGURE 3-3

other variables. This agrees with fuel cell theory as discussed by Adams, Bacon, and Watson.⁽⁴⁾ An increase in pressure raises the reversible potential and may also reduce activation polarization by increasing the exchange currents.

The magnitude of the pressure effect increased with increasing current density. This is to be expected. Higher pressure, which increases the solubility of the gases in the electrolyte, reduces polarization caused by gas diffusion limitations which are more significant at higher current densities.

The magnitude of the pressure effect tended to diminish with increasing pressure, particularly at high current densities. In general, however, the voltage at all current densities was substantially higher at 60 psig than at 30 psig.

3.2.2 Temperature

The effects of temperature and KOH concentration were interdependent. Both the direction and magnitude of these effects depended on current density and on how close the KOH concentration was to the solubility limit.

The effect on performance of increasing the temperature in the range 100-150°C is shown in Figure 3-4. Pressures were 15, 30 and 60 psig. KOH concentrations were 30%, 45% and 60%. Voltages are illustrated at 100, 400, and 1000 ma/cm². The solubility limit of KOH is 65% at 100°, 70% at 125°C, and 80% at 150°C.⁽⁵⁾ Thus 30% KOH is 35, 40, and 50% below the solubility limit, 45% KOH is 20, 25, and 35% below, while 60% KOH is only 5, 10 and 20% below the solubility limit at 100, 125, and 150°C, respectively.

EFFECT OF TEMPERATURE ON PERFORMANCE

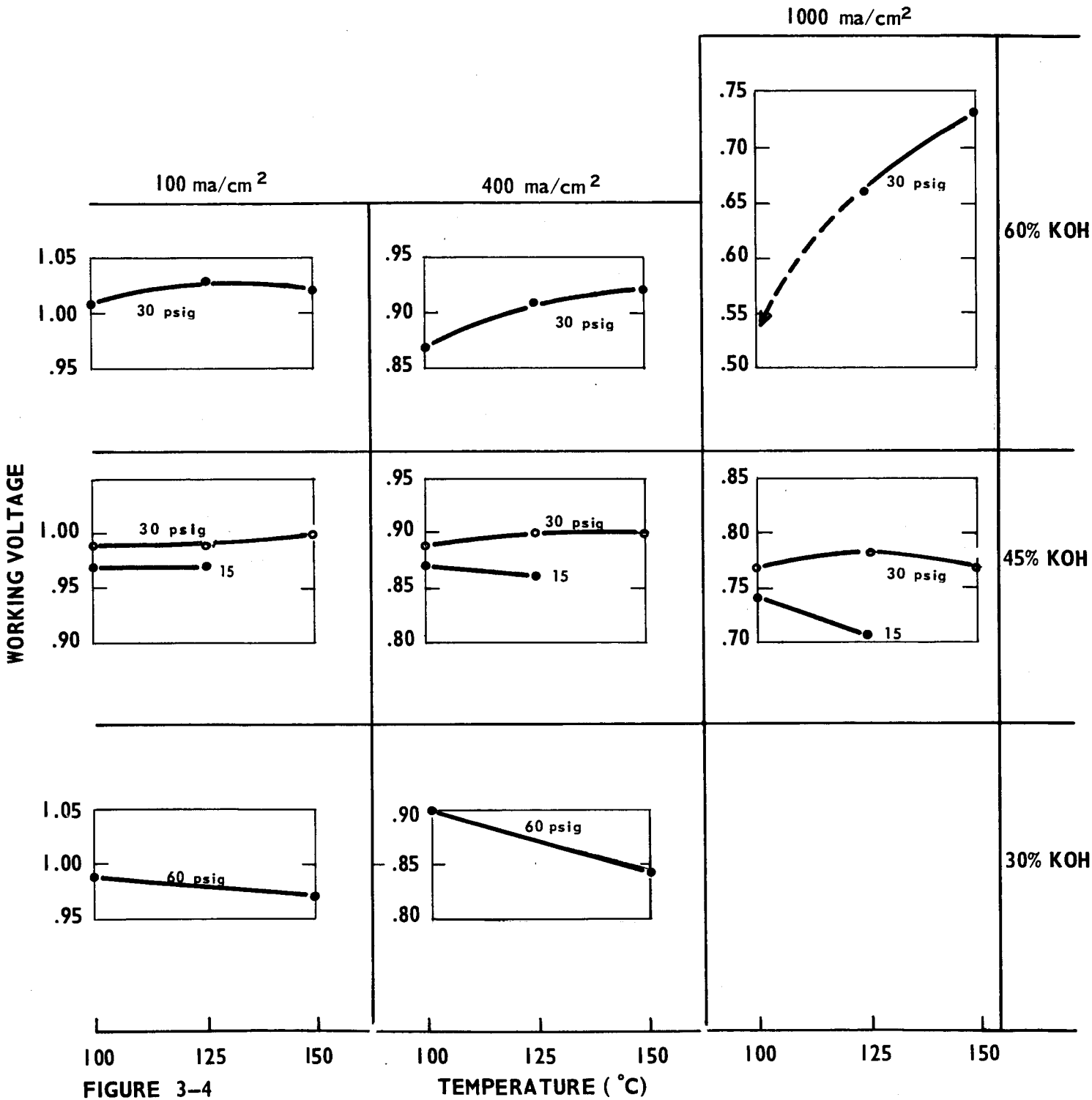


FIGURE 3-4

TEMPERATURE (°C)

At 30% and 45% KOH, increasing the temperature from 100 to 150°C had little effect on performance over the entire range of current density. By contrast, at 60% KOH, performance increased substantially with increasing temperature. The magnitude of this temperature effect was greater at the higher current densities. Thus at 100 ma/cm², an increase from 100 to 125°C raised the voltage while a further increase to 150°C did not. However, at 400 ma/cm², the voltage increased over the whole temperature range. At 1000 ma/cm², the initial voltage was unstable at 100°C, stable at 125°C and further improved at 150°C.

It appears that increasing the temperature in the range 100-150°C improves performance only at KOH concentrations close to the solubility limit, and that under these conditions, the improvement is greater at the higher current densities. Thus with these high-loading electrodes, the principal effect of increasing the temperature in this range is probably the reduction of polarizations associated with electrolyte or gas diffusion limitations.

3.2.3 KOH Concentration

The effect of KOH concentration on performance is shown in Figure 3-5. At each temperature, the highest concentration shown is 5% below the solubility limit. It can be seen that the effect of concentration depends on both current density and temperature. At 100 ma/cm², increasing the KOH concentration to within 5% of the solubility limit increased the voltage markedly at all temperatures in the range 100-150°C. At higher current densities, voltage increases were obtained at all temperatures as the KOH concentration was increased from 30% to 45%.

EFFECT OF KOH CONCENTRATION ON PERFORMANCE

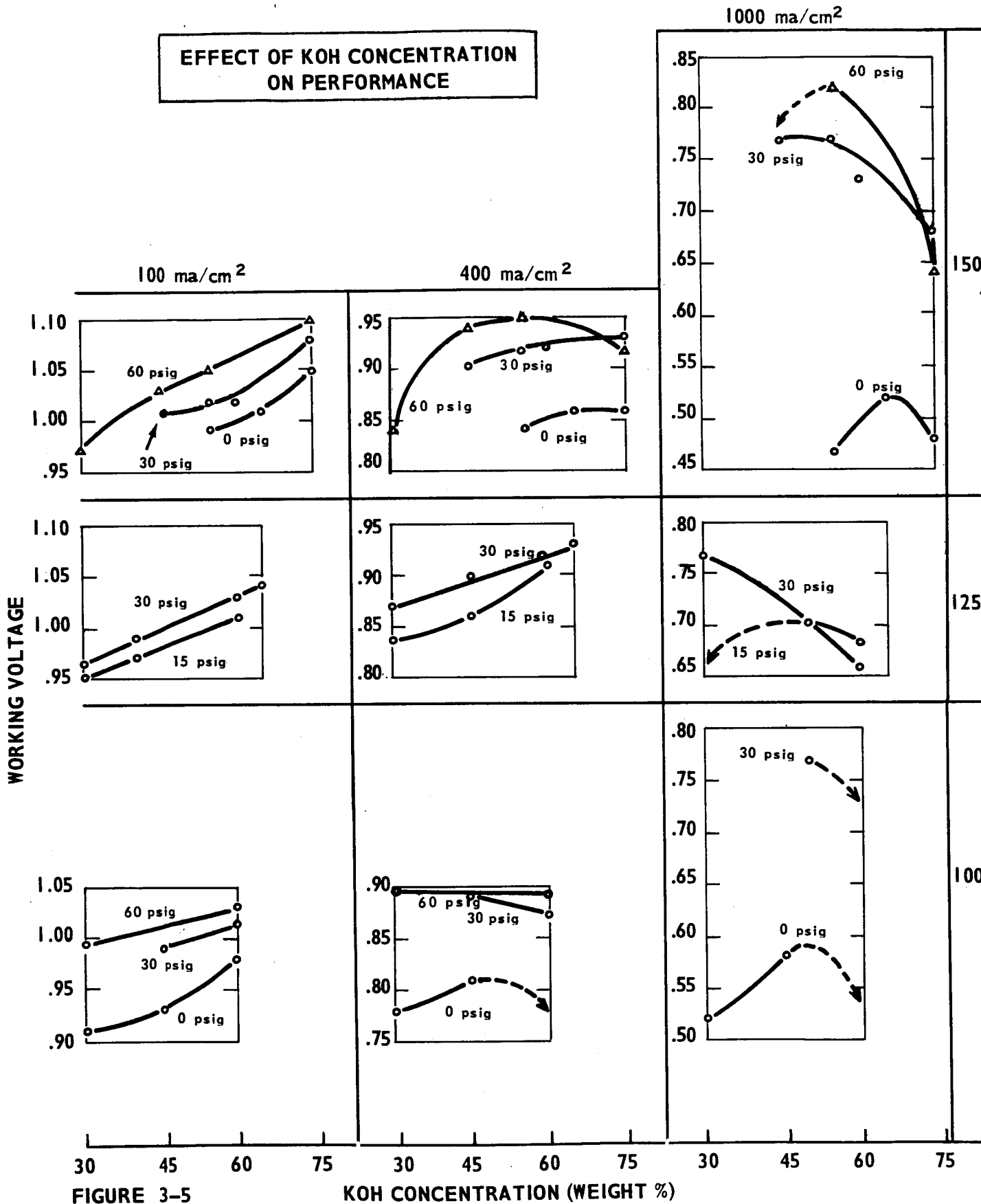


FIGURE 3-5

KOH CONCENTRATION (WEIGHT %)

As the concentration was further increased however, performance decreases were observed in some cases. The concentration yielding maximum performance ranged from 5 to 25% below the solubility limit, and in general was further below the solubility limit at higher than at lower current densities.

3.2.4 Regions of Unstable Operation

In a few runs in the vicinity of the solubility limit, e.g., at 100°C and 60% KOH, the initial voltage was unstable at current densities greater than 200-400 ma/cm². Unstable performance also occurred when the partial pressure of water was substantially above atmospheric. Thus in the run at 150°C, 30% KOH, the partial pressure of water was 2300 mm⁽⁶⁾ and the voltage was unstable at current densities above 200 ma/cm². At a partial pressure of 1100 mm (150°C, - 45% KOH and 125°C - 30% KOH) voltages were unstable at current densities above 600-800 ma/cm². At all lower partial pressures down to 50-100 mm, in the vicinity of the solubility limit, the initial voltage was stable at all current densities.

3.2.5 Highest Performance Levels

At all current densities the best performance was obtained at the maximum levels of temperature and pressure investigated, i.e., 150°C and 60 psig. At 100 and 200 ma/cm² the highest voltages were 1.10 and 1.03 v, respectively. They were obtained at 75% KOH, the highest concentration employed. At 300 ma/cm² the highest voltage (0.98 v) was obtained with both 75% and 55% KOH. At greater current densities, 55% KOH gave the best performance. Highest voltages at 400, 600, 800, and 1000 ma/cm² were 0.95, 0.91, 0.86, and 0.82 v, respectively.

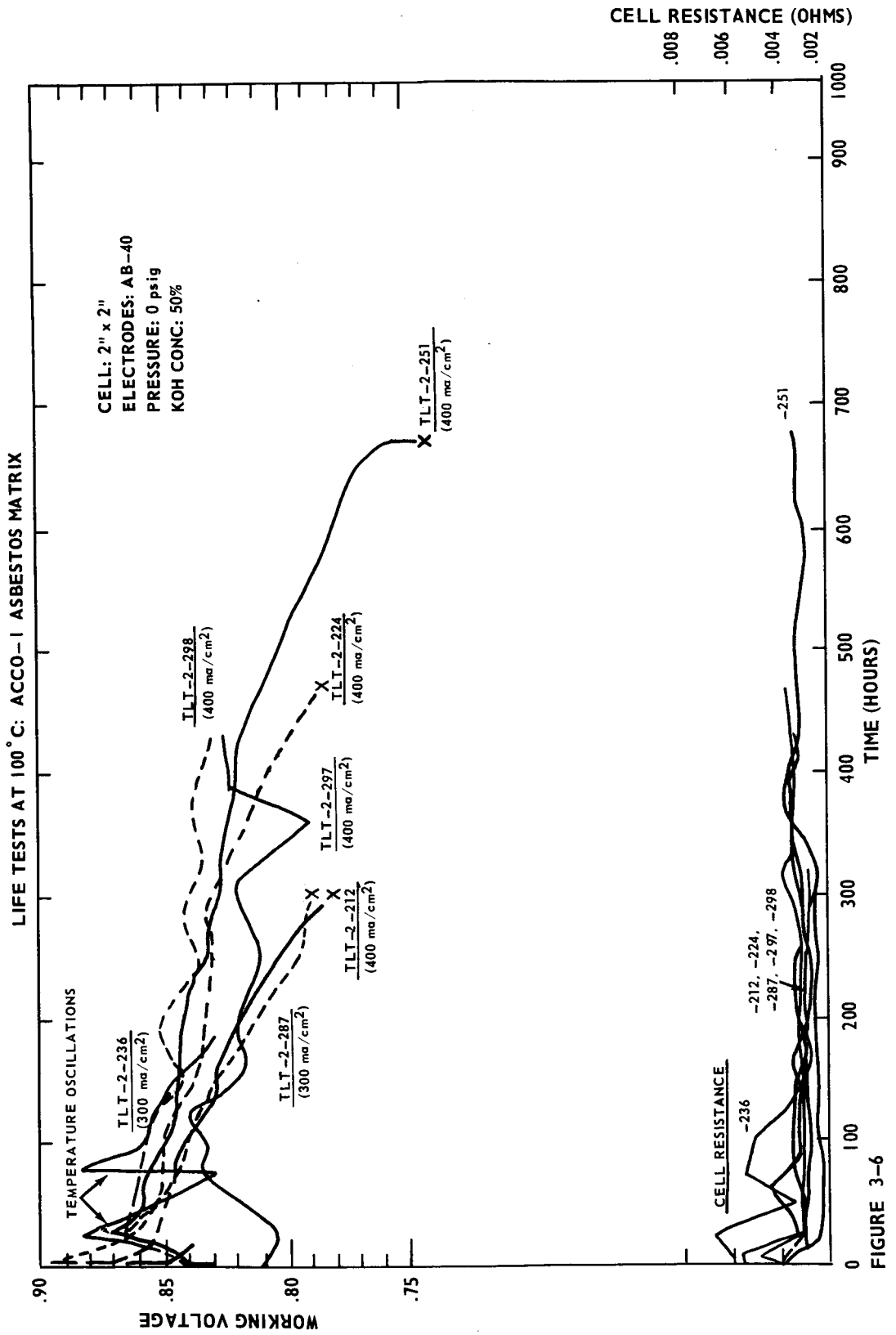


FIGURE 3-6

LIFE TESTS AT 100° C.: ACCO -II ASBESTOS MATRIX

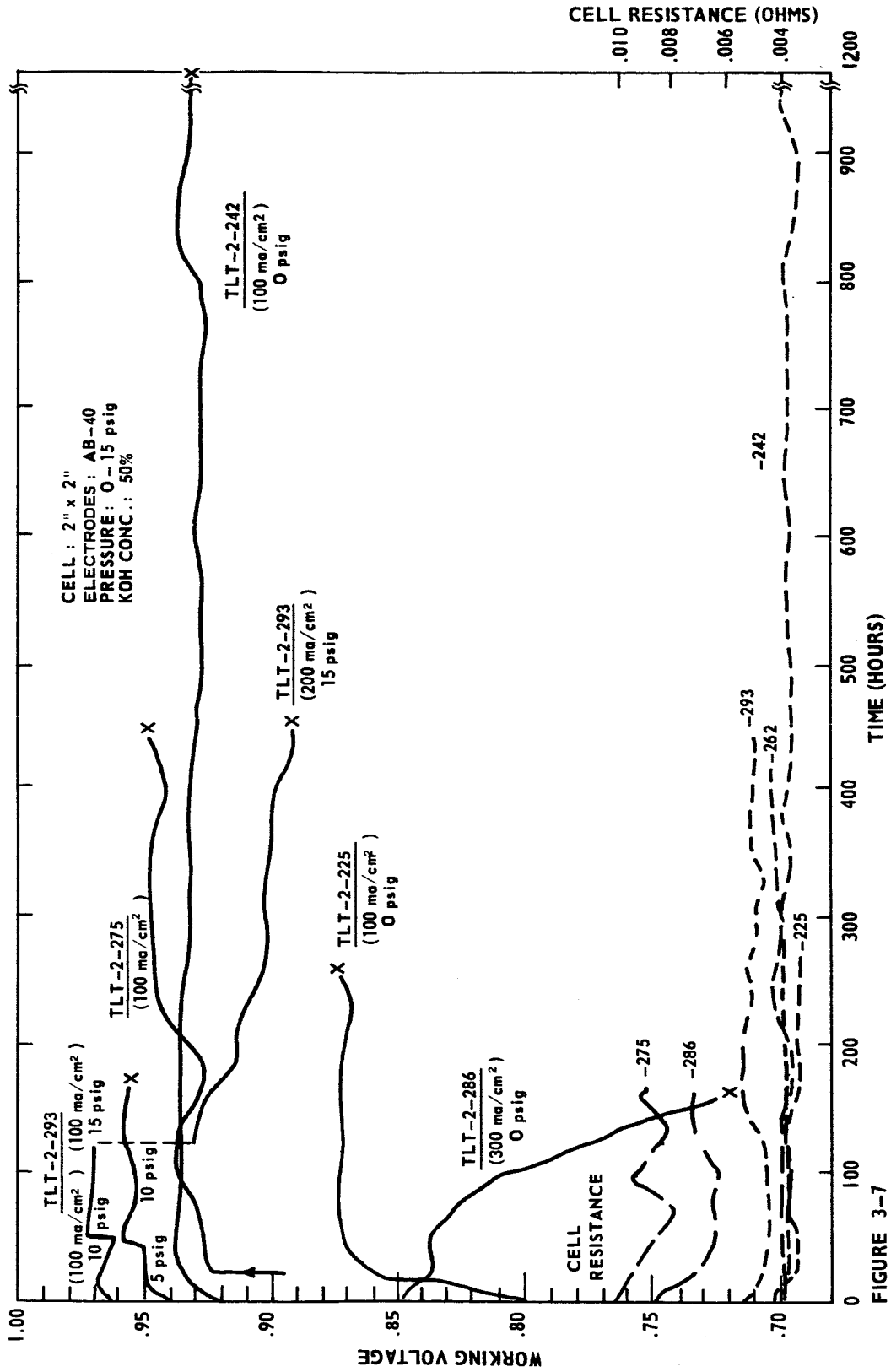


FIGURE 3-7

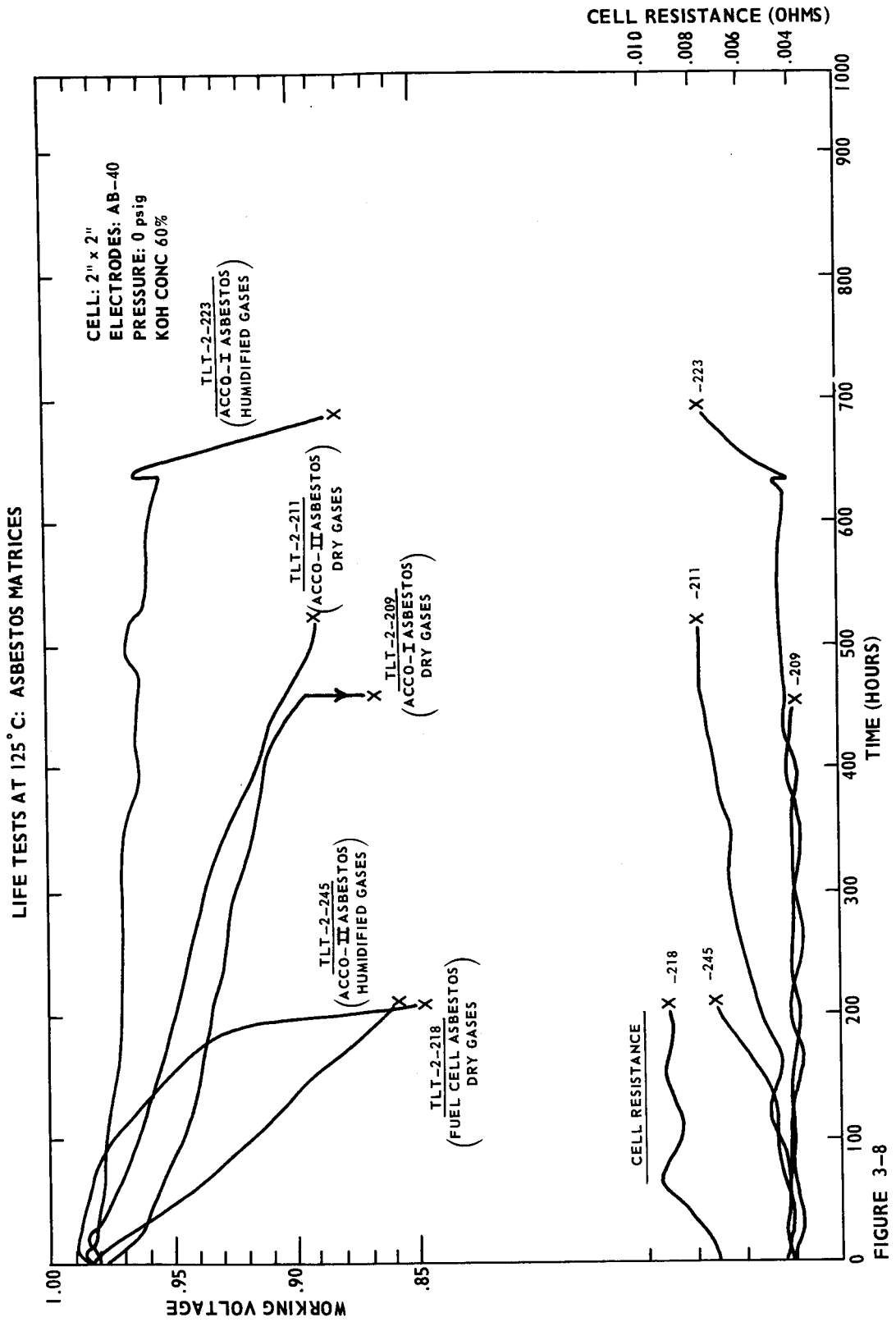


FIGURE 3-8

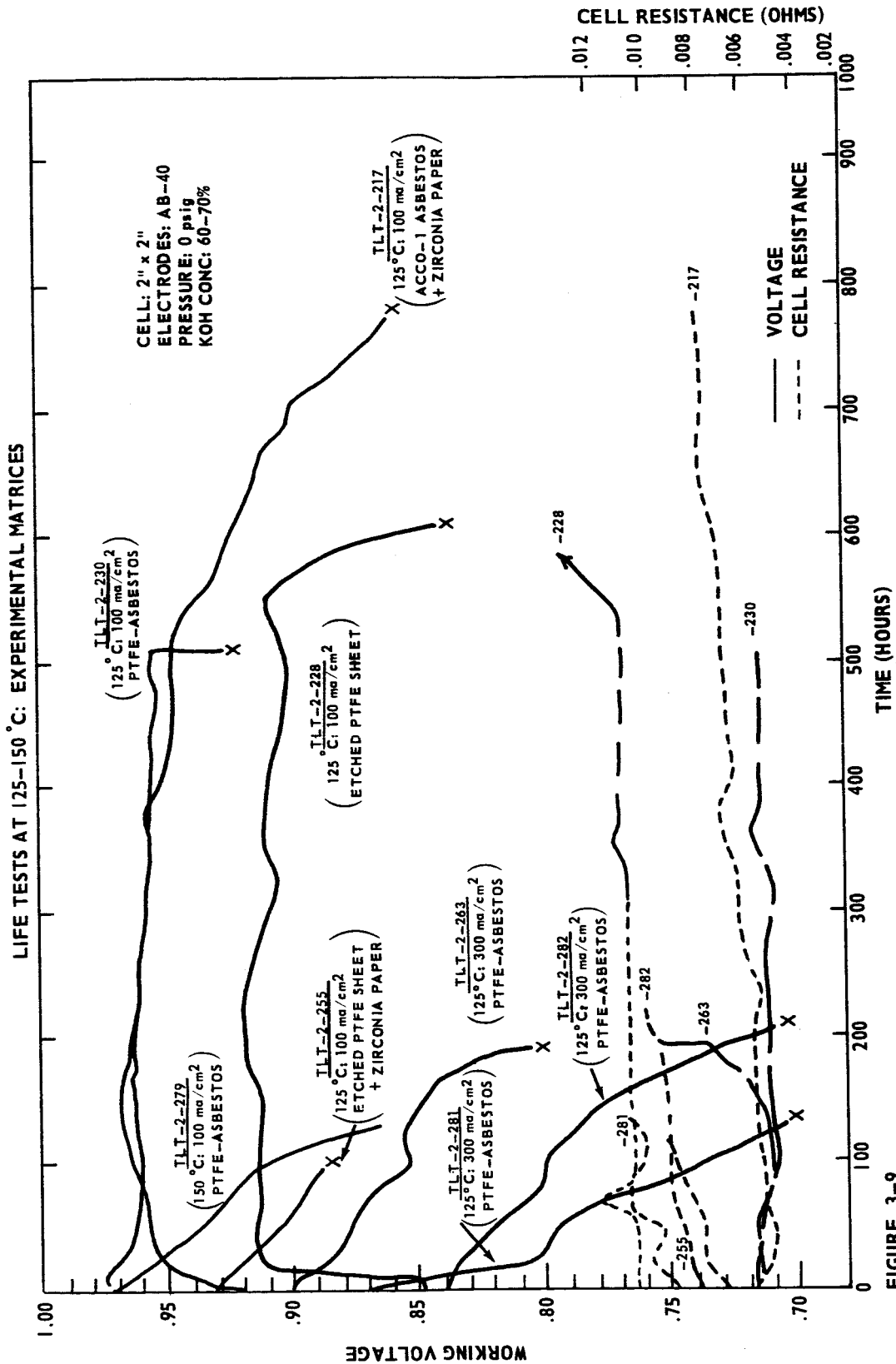


FIGURE 3-9

TABLE 3-5
Life Tests: 2" x 2" Cells: 100°C (a)

TIT No.	Matrix	Matrix Thickness (Mils)	Current Density (mA/cm ²)	KOH Conc. (g)	KOH Loading (g/g Matrix)	Inlet Gas Condition	Inlet Gas Flow Rates		Inlet Flow Ratio (H ₂ /O ₂)	Test Duration (Hrs.)	Working Voltage		Cell Resistance (Milliohms)		Overall Voltage Decline Rate (mv/100 Hrs.)	Status	Reason For Termination
							cc/min at 23°C	O ₂			Initial	Maximum	Initial	Maximum			
2-287	ACCO-I Asbestos	25	300	50	3.1	Dry	307	77	4.0	305	.873	.873	5.0	3.2	3.4	Terminated	(1)
2-236	"	"	400	"	"	"	192	192	1.0	187	.468	.889	4.0	3.0	3.0	Continuing	-
2-212	"	"	"	"	"	"	192	192	"	306	.193	.778	3.0	2.9	3.0	Terminated	(1)
2-224	"	"	"	"	"	"	230	194	1.5	453	.800	.900	4.2	3.0	3.5	"	"
2-297	"	"	"	"	"	"	128	296	0.5	432	.810	.842	3.5	3.1	3.5	Continuing	-
2-244	"	"	"	"	"	"	192	192	1.0	20	.331	.785	4.4	3.4	4.0	Terminated	(2)
2-251	"	"	"	"	"	"	288	96	3.0	669	.867	.880	6.0	2.9	3.0	"	(3)
2-298	"	"	"	"	"	Humidified at 40°C	246	246	1.0	430	.683	.867	6.2	2.8	3.6	Continuing	-
2-247 (d)	"	"	"	"	"	Dry	192	192	"	68	.810	.810	7.0	6.0	6.0	Terminated	(4)
2-249 (d)	"	"	"	"	"	"	292	292	"	48	.816	.816	5.6	5.6	7.0	"	"
2-225	ACCO-II Asbestos	20	100	"	2.5	"	51	45	1.1	257	.750	.873	4.5	3.2	3.2	"	"
2-240	"	"	"	"	3.1	"	51	45	"	113	.534	.956	4.0	3.5	3.6	"	(1)
2-242	"	"	"	"	2.0	"	51	45	"	1200	.925	.938	4.0	3.5	3.5	"	"
2-286	"	"	300	"	2.7	"	144	144	1.0	165	.848	.848	9.0	6.5	7.5	"	"
2-262 (d,e)	"	"	100	50 → 54	"	"	68	64	1.1	451	.800	.950	4.0	3.6	4.5	"	"
2-277 (b,d,e)	"	"	"	50	"	"	63	63	1.0	169	.940	.950	10.5	8.0	9.3	"	(5)
2-293 (c)	"	"	100	"	1.7	"	77	77	"	454	.964	.972	5.5	4.2	4.4	"	"
			200	"	"	"	184	184	"		.929	.930	5.2	4.5	4.8	Continuing	(6)

TABLE 3-5 (Continued)
Life Tests: 2" x 2" Cells: 125°C

T/F No.	Matrix	Thickness (Mils)	Current Density (ma/cm ²)	KOH Conc. (%)	KOH Loading (g/g Matrix)	Inlet Gas Condition	Inlet Gas Flow Rates cc/min at 0 psi at 125°C	Inlet Flow Ratio (D ₂ /O ₂)	Test Duration (hrs.)	Working Voltage		Overall Voltage Decline Rate (mv/100 hrs.)	Cell Resistance (Milliohms)		Status	Reason for Termination
										Initial	Maximum		Initial	Minimum		
2-209	ACCO-I Asbestos	25	100	60	3.0	Dry	40	1.0	477	.930	.972	16	4.0	4.0	Terminated	(4)
2-223	" "	"	"	"	4.0	Humidified at 55°C	128	0.67	689	.926	.989	4 (f)	4.2	3.6	"	"
2-211	ACCO-II Asbestos	20	"	"	3.1	Dry	50	1.0	522	.939	.989	18	4.2	4.2	"	(1)
2-245	" "	"	"	"	2.7	Humidified at 55°C	128	0.67	209	.850	.987	Accelerated	4.4	4.0	"	(7)
2-218	Fuel Cell Asbestos	"	"	"	1.5	Dry	50	1.0	210	.947	.984	58	7.0	7.0	"	(1)
2-213	Zirconia Paper	3 x 30	"	"	5.7	"	50	"	18	.302	.808	320	-	-	"	(4)
	" "	5 x 30	"	"	3.0	"	"	"	1	.525	.876	-	-	-	"	"
2-230	PIFE Asbestos	15	"	"	-	"	50	50	524	.875	.978	3 (f)	5.5	4.8	"	"
2-282	" "	24	300	"	1.1	"	100	0.5	263	.783	.841	70 (f)	6.6	7.5	"	(1)
2-263	" "	15	"	"	1.0	"	150	1.0	210	.830	.900	36 (f)	5.5	4.0	"	(7)
2-261	" "	24	"	"	1.1	"	200	2.0	142	.861	.874	120	8.5	8.5	"	(1)
2-219	PINK-Zirconia	25	100	"	0.65	"	50	1.0	17	.146	.146	0.4	10.1	7.2	"	(4)
2-239	" "	"	"	"	5.8	"	50	50	65	.832	.953	535	4.0	3.4	"	"
2-229	Etched PTFE Felt (g)	30	"	"	-	"	50	50	16	.773	-	Accelerated	3.0	-	"	"
2-257	" "	60	"	"	1.2	"	50	50	15	.865	.930	-	7.5	7.5	"	(7)
2-272	" "	20	"	"	1.6	"	63	63	93	.160	.869	-	8.8	8.2	"	"
2-256	Etched PTFE Sheet (h)	10	"	"	2.6	"	50	50	43	.880	.968	190	5.5	5.5	"	"
2-228	" "	20	"	"	1.3	"	50	50	667	.788	.918	2 (f)	10.5	10.1	"	(4)
2-221	" "	32	"	"	0.57	"	50	50	0.2	-	-	-	-	-	"	(3)
2-217	ACCO-I Asbestos + Zirconia Paper	85	"	"	3.1	"	50	50	788	.750	.968	54	5.5	4.8	"	(1)
2-275	Etched PTFE Sheet (h) + Zirconia Paper	40	"	"	3.3	"	50	50	113	.710	.932	40	8.0	8.0	"	(7)

TABLE 3-5 (Continued)

Life Tests: 2" x 2" Cells: 150°C

TUP No.	Matrix	Thickness (mils)	Current Density (mA/cm ²)	KOH Conc. (%)	KOH Loading (g/g Matrix)	Inlet Gas Condition	Inlet Gas Flow Rates (cc/min at 23°C)		Inlet Flow Rate (H ₂ /O ₂)	Test Duration (Hrs.)	Working Voltage		Overall Voltage Decline Rate (mv/100 Hrs.)	Cell Resistance (Milliohms)		Status	Reason For Termination
							H ₂	O ₂			Initial	Maximum		Initial	Final		
2-265	ACCO-I Asbestos	25	100	70	4.0	Humidified at 55°C	150	150	1.0	16	.966	1.000	> 200	5.3	14.5	Terminated	(7)
2-270	PIFE-Asbestos	12	"	"	0.9	Dry	63	63	"	68	.946	.987	> 200	5.5	5.6	"	"
2-267	"	"	"	"	1.3	"	63	63	"	66	.918	1.000	> 200	5.0	5.5	"	"
2-279	"	24	"	60	1.1	"	50	50	"	137	.923	.973	> 60	8.5	21.8	"	"
2-289	Etched PTFE Sheet (1)	20	"	"	1.0	"	63	63	"	1	.943	.943	-	10.7	-	"	"
2-290	"	"	"	"	1.1	Humidified at 67°C	50	50	"	8	.911	.911	-	-	-	"	"

GENERAL NOTES

- (a) All tests use pre-wet AB-40 electrodes and H₂ and O₂ at 0 psig unless noted otherwise
- (b) 5 psig - then 10 psig H₂ and O₂
- (c) 10 psig - then 15 psig H₂ and O₂
- (d) Dry electrodes
- (e) Pressure cell used at 0 psig to check performance
- (f) Prior to abrupt voltage decline due to cross leakage of gas
- (g) American Velt Company
- (h) Chemcell Inc.
- (i) 5% KOH initially charged/g dry matrix. In tests at 12°C and 150°C where the electrolyte was concentrated in the cell to 60% and 70%, the final loading is proportionately lower.

REASONS FOR TERMINATION

- (1) Voltage decline rate defined
- (2) Low voltage level
- (3) Oxygen off accidentally
- (4) Gas cross-leakage
- (5) Faulty pressure controller
- (6) Transfer to new lab
- (7) Extremely rapid voltage decline
- (8) Electrode-electrode contact

3.3 Life-Testing

Small cell life tests were run at temperatures up to 150°C, KOH concentrations up to 70%, pressures up to 15 psig, and current densities as high as 400 ma/cm².

These matrices included several types of asbestos, zirconia paper, PTFE felt and sheet, PTFE-asbestos, and PTFE-zirconia. Pre-wet electrodes were used in all tests but three. The inlet gases were either both dry or both humidified. The KOH loading and the H₂/O₂ flow ratio were varied. Inlet gas flow rates ranged from 45-307 cc/min. Test conditions and results are summarized in Table 3-5. Changes of cell voltage and resistance with time are shown in Figures 3-6 to 3-9 for all tests which ran more than 100 hours. The mode of failure, or reason for termination, is given in Table 3-5 for each test. In some cases, termination was forced due to equipment difficulties, or to internal cell problems such as cross-leakage of gases. In other cases, tests were terminated arbitrarily because maximum voltages were too low or decline rates too high.

3.3.1 Tests at 100°C

Tests at 100°C and 50% KOH were made with both ACCO-I and ACCO-II Asbestos. Figure 3-6 shows voltage-time and resistance-time curves for ACCO-I Asbestos. During the first quarter, it was reported⁽²⁾ that life tests with ACCO-I Asbestos containing 50% KOH ran stably at current densities up to 300 ma/cm². The lowest voltage decline rates at 100, 200 and 300 ma/cm² were 0.6, 3.2 and 4.2 mv/100 hours, respectively.

The test at 300 ma/cm² (TLT-2-208) had been run with dry gases at an inlet H₂/O₂ ratio of 1.0. During the current period a run was made with an inlet H₂/O₂ ratio of 4.0 (TLT-2-287), in order to determine the effect of such a high ratio. The voltage decline rate was very high (25 mv/100 hours).

Acceptable stability has not yet been achieved at 400 ma/cm². Tests with dry electrodes (TLT-2-247) and -249) quickly developed cross-leakage of gas within less than 100 hours and had to be terminated. Cross-leakage was evident from an immediate and precipitous voltage drop when (during flow measurements) a pressure differential of only two inches of water occurred across the matrix. With pre-wet electrodes the voltage decline rate (22-44 mv/100 hrs.) were high over a wide range of inlet H₂/O₂ ratios, 0.5-3.0 (TLT-2-297, -212, -236, -224, and -251). The decline rates at flow ratios of 1.5-3.0 (22-25 mv/100 hrs.) were lower than at a flow ratio of 1.0 (32-44 mv/100 hrs.) However, at a flow ratio of 0.5 (TLT-2-297) the voltage after 432 hours (0.828) was only 14 mv below the maximum voltage (0.842). This drop is much lower than those encountered at higher flow ratios. Accordingly, the effect of flow ratio is not yet clear. Much more stable performance at 400 ma/cm² and an H₂/O₂ ratio of 1.0 was achieved by humidifying the inlet gases at 40°C (TLT-2-298). The maximum voltage was 0.867. During 400 hours the voltage decline rate was 8 mv/100 hours, considerably less than in the runs with dry gases at the same flow ratio (TLT-2-212 and -236). Thus it appears that drying out of the electrodes at local points may contribute to the high voltage decline rates at this high current density. In principle, humidification at 40°C prevents the concentration at any point on the electrode from exceeding 62 1/2% (only 2 1/2% below the solubility limit). Higher humidifier temperature may produce better voltage stability by lowering the maximum possible KOH concentration. Some evidence for this was found in large cell life testing and is discussed further in Section 5.2.

ACCO-II Asbestos was included in the life testing program because it has sufficient bubble pressure (20 psig) for life testing under pressure. All runs were made with dry gases. Voltage-time and resistance-time curves are shown in Figure 3-7. At atmospheric pressure, acceptable performance stability was achieved in a 1200 hour test at 100 ma/cm² (TLT-2-242). The final voltage was 0.93 v. TLT-225 ran at a low voltage level (0.87 v). TLT-2-240 at 100 ma/cm² and TLT-2-286 at 300 ma/cm² had high voltage decline rates.

Life tests at 0-15 psig were run with ACCO-II Asbestos in the cell designed for pressures above atmospheric. Test TLT-2-262 was run at 0 psig and 100 ma/cm² as a general check of the cell. The electrodes were assembled dry. The low initial voltage (0.80 v) may have been due to an initial shorting of the cell with the pins used to align the face plates. The flow rates were inadvertently set too high, causing the electrolyte to concentrate to 54%. This increase in concentration probably accounts for the somewhat higher level of performance reached in this test. Performance was extremely stable during 451 hours. The voltage decline rate was zero. TLT-2-275 was run at 100 ma/cm² with the hydrogen and oxygen at 5 psig. The cell resistance was abnormally high (10.5 milliohms as compared with 4-5 milliohms usually obtained with this matrix). Nevertheless the maximum voltage (0.950 v) was 12 mv above that at 0 psig (TLT-2-242). The cell operated stably for 45 hours, at which time the pressure was increased to 10 psig. The voltage rose to 0.960 v, but a slight voltage and resistance oscillation was induced. Shutdown was forced at 169 hours by a faulty pressure controller. Test TLT-2-293 was started at 10 psig and 100 ma/cm².

The initial resistance (5.5 milliohms) was normal. Accordingly the maximum voltage (0.972 v) was 12 mv above that in run TLT-2-275 and 34 mv above the test at 0 psig. As with the previous test, some instability was noted in the voltage. After 47 hours the pressure was increased to 15 psig. The voltage increased by 10 mv but this was only 5 mv above the maximum voltage reached at 10 psig. At 15 psig the voltage declined at about 3 mv/100 hr during 73 hours. At 120 hours total elapsed time the current density was increased to 200 ma/cm². At this current density the decline rate was high (10 mv/100 hrs.).

3.3.2 Tests at 125°C

All tests at 125°C were run at atmospheric pressure and, except for three tests with the PTFE-Asbestos matrix, at a current density of 100 ma/cm². The electrolyte was loaded at 50% and then concentrated in the cell to 60%. Figure 3-8 shows the change of voltage and resistance with time for tests with ACCO-I Asbestos, ACCO-II Asbestos and Fuel Cell Asbestos matrices.

With ACCO-I Asbestos maximum voltages of 0.97-0.99 v were reached. Operation with dry gases, at an H₂/O₂ inlet ratio of 1.0, and a KOH loading of 3.0 g/g dry matrix gave a high voltage decline rate of 16 mv/100 hrs. (TLT-2-209). Operation with gases humidified at 55°C, at an H₂/O₂ ratio of 0.67, and a KOH loading of 4.0 g/g yielded stable operation for 640 hours in test TLT-2-223. The decline rate during this period was 4 mv/100 hrs. After 640 hours, the voltage declined rapidly due to cross-leakage of gas. The most probable cause of cross-leakage was dissolution of some asbestos by the KOH.

ACCO-II Asbestos (TLT-2-211) operating on dry gases under the same conditions as ACCO-I Asbestos (TLT-2-209) gave approximately the same high voltage decline rate (18 mv/100 hrs). Operation with the gases humidified at 55°C (TLT-2-245) gave an accelerated decline rate.

Fuel Cell Asbestos which ran poorly at 100°C also showed poor stability at 125°C on dry gases, with a voltage decline rate of 58 mv/100 hrs. (TLT-2-218).

Figure 3-9 shows the results of life tests lasting more than 100 hours with matrices of PTFE-Asbestos and PTFE sheet. Also shown are runs with laminated composite matrices of ACCO-I Asbestos-zirconia paper and PTFE sheet-zirconia paper. Shorter tests with these matrices and with zirconia paper, PTFE felt and PTFE-zirconia sheet are listed in Table 3-5, but not shown in the figure. All runs were made with dry gases.

As reported previously⁽²⁾ an experimental proprietary PTFE-Asbestos matrix is available. The matrix contains 75% PTFE by weight and was devised to have greater overall chemical stability than asbestos alone while retaining a suitably low resistance. A 15 mil thickness of this matrix yielded a minimum cell resistance of 4.8 milliohms and a maximum voltage at 100 ma/cm², of 0.98 (TLT-2-230). On dry gases, the voltage decline rate was 3 mv/100 hrs. during 490 hours. This was as low as that of ACCO-I Asbestos on humidified gases. After 490 hours cross-leakage developed, however. The voltage declined rapidly and the test was terminated. At 300 ma/cm², a 15 mil thick matrix gave a maximum voltage of 0.90 v (TLT-2-263). During 160 hours, the voltage decline rate was high (38 mv/100 hrs.). This was followed by an abrupt decline accompanied by a rapid rise in resistance, indicating possible water balance problems. In this run the inlet H₂/O₂ flow ratio was 1.0. Runs were made at flow ratios of 0.5 and 2.0 with 24 mil thick matrices (TLT-2-282 and -281). These matrices yielded higher resistance and lower maximum performance, 0.841 v and 0.874 v, than the 15 mil matrix. Voltage decline rates were very high in both tests.

Zirconia paper (H. I. Thompson Company) was used as a matrix in life test TLT-2-213. The cell was first set up with three 30-mil sheets then restarted with five sheets. This material has an extremely high void volume (96%) with macroscopic pores. Consequently considerable cross-leakage of gas and extremely rapid voltage decline rates were observed (320 mv/100 hrs. during an 18 hour period for the first test). To overcome cross-leakage, a sheet of ACCO-I Asbestos was sandwiched between two sheets of Zirconia Paper (TLT-2-217). In this test the voltage rose slowly to a maximum during the first 170 hours, was relatively stable up to 520 hours, and then declined rapidly during the next 140 hours.

An experimental 50/50 PTFE-Zirconia matrix obtained from Chemcell Incorporated was evaluated in runs TLT-2-219 and -239. When loaded with 5.8 times its own weight of KOH this matrix gave an acceptable resistance (4.0 milliohms). Again however, considerable difficulty was encountered with cross-leakage of gases. In run TLT-2-219, cross-leakage occurred at the start and the voltage did not rise above 0.15v. In run TLT-2-239 a maximum voltage of 0.95v was reached but declined rapidly during 65 hours.

Cross-leakage was also encountered with a matrix made from PTFE Felt (American Felt Company) which had been etched to improve its wettability. Rapid voltage decline rates were observed in three tests with this matrix.

Two grades of etched porous PTFE sheet (Chemcell, Incorporated) were evaluated as matrices. Grade W4-125 is 5 mils thick and has an average pore size of 5 microns. Grade 233WS is 16 mils thick and has an average pore size of 20 microns. Both grades have an available void volume of approximately 65%. In preliminary tests⁽²⁾ with these materials, it was found that because of hot flow of the PTFE the electrodes tended to break through the matrix and short-circuit the cell. In the life-testing program,

multiple layers of these matrix materials were used in an effort to overcome this problem. TLT-2-221, employing two sheets of 233 WS, was terminated within fifteen minutes because of electrode-electrode contact. Four sheets of W4-125 were used in TLT-2-228. In this test, 0.01% FC-95 (a 3-M Company perfluorinated surfactant) was added to the electrolyte to help wet the matrix. Cell resistance was relatively high (10.1 milliohms) and maximum voltage correspondingly low (0.918 v). Reasonably stable performance was maintained for a period of 540 hours (overall voltage decline rate of 2 mv/100 hrs.). Cell resistance did not change significantly during this period. After 540 hours, cross-leakage of gas developed, the voltage declined rapidly, and the cell resistance simultaneously rose rapidly. This run demonstrated that porous PTFE sheet can be wet sufficiently to give sustained performance for at least 500 hours. Examination of the matrix after test showed, however, that the etched surface is not stable under these conditions. The surface, normally brown, was bleached to an off-white color, and was no longer wetted by 50% KOH. Loss of wettability may have caused the electrolyte to become discontinuous, thus permitting both cross-leakage of gas and an increase in the cell resistance. The use of FC-128, which lowers the surface tension of KOH more than does FC-95, might be helpful in maintaining the wettability of this type of matrix.

Based on the life-test results discussed in this section, it appears that none of the matrix materials evaluated is adequate in terms of sustained high level performance at 125°C.

3.3.3 Tests at 150°C

At 150°C, 60-70% KOH and 100 ma/cm² both ACCO-I Asbestos and PTFE-Asbestos gave extremely unstable performance. Voltage decline rates were

generally greater than 200 mv/100 hrs. and were accompanied by rapid rises in cell resistance (TLT-2-265, -267, -270 and -279). The rapid resistance rise was probably due to solution of the asbestos in the electrolyte.

3.3.4 Polarization Data on Used Electrodes

In order to help determine the location and cause of losses in performance during life tests, polarization curves were run with various combinations of new and used electrodes. The used discs, 1" in diameter, were cut from 2" x 2" life-tested electrodes and then washed and dried. The asbestos matrix used in life-testing could not be removed completely from the matrix side of these discs. Consequently, the discs were placed with their gas side as well as their matrix side (from the life test) against the matrix used in the polarization runs, to determine whether occluded asbestos affects electrode performance.

Figure 3-10 shows the results for the electrodes used in run TLT-2-198 at 125°C. In this test, using ACCO-I Asbestos, the voltage had declined by 80 mv during 618 hours. All polarization runs in which at least one used electrode was employed show poorer performance than the run with two new electrodes.

The voltage loss of each curve at 300 ma/cm² (arbitrary) was measured, relative to the new electrode curve, and a voltage loss assigned to each electrode face as shown below.

<u>Voltage Loss Assignments</u>		
<u>Electrode</u>	<u>Matrix Side</u>	<u>Gas Side</u>
H ₂	96	96
O ₂	38	60
H ₂ + O ₂ Sum	134	156
H ₂ + O ₂ Measured	258	96

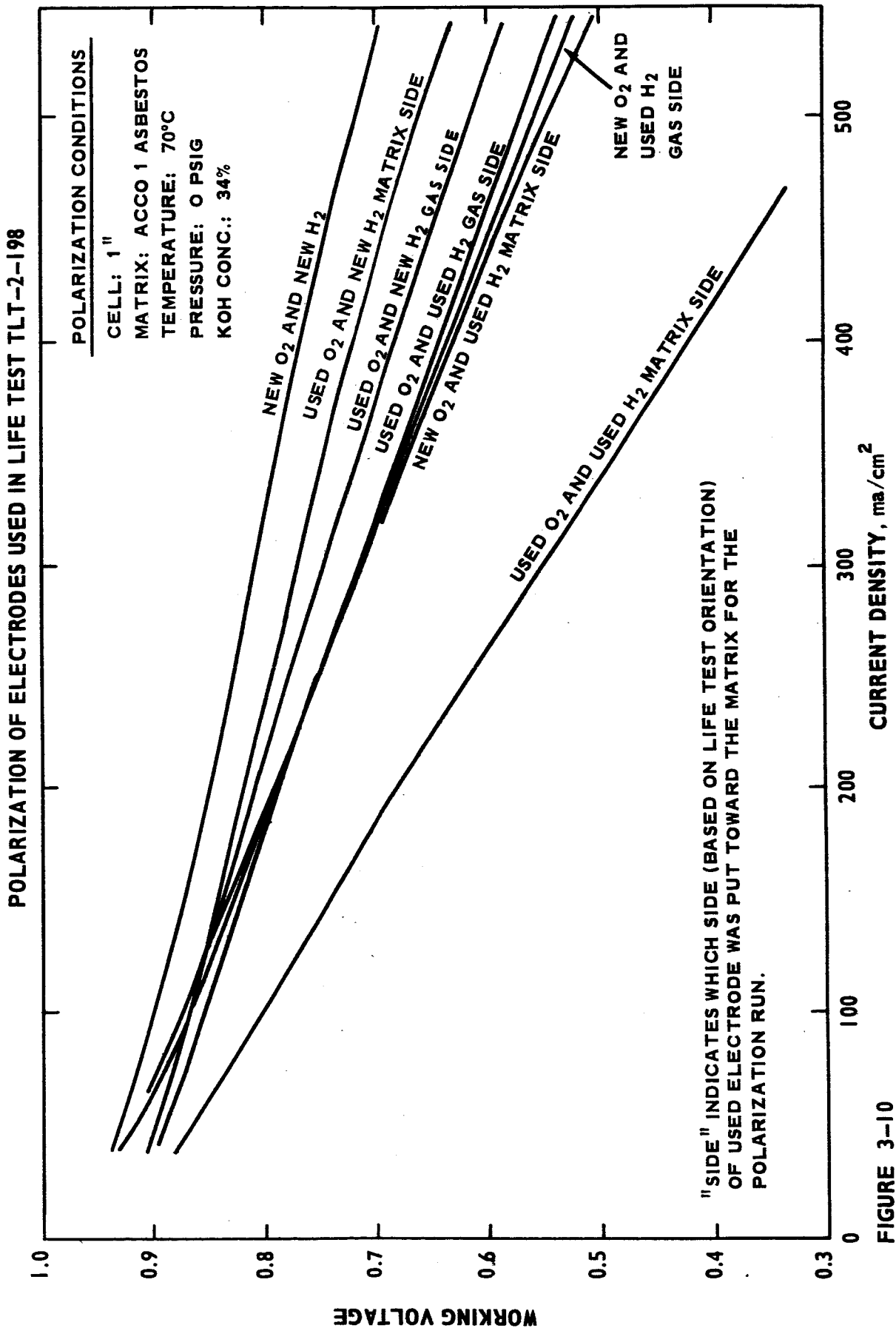


FIGURE 3-10

As can be seen from the last two rows inconsistencies develop in the analysis. A possible cause was the use of the electrode discs for more than one polarization curve.

A similar series of runs was made with the electrodes from life test TLT-2-206 (125°C for 521 hours, ACCO-I matrix). The curves fall in the same sequence except for the used O₂-new H₂-matrix side curve which was unexplainably low (below the used O₂-used H₂-matrix side).

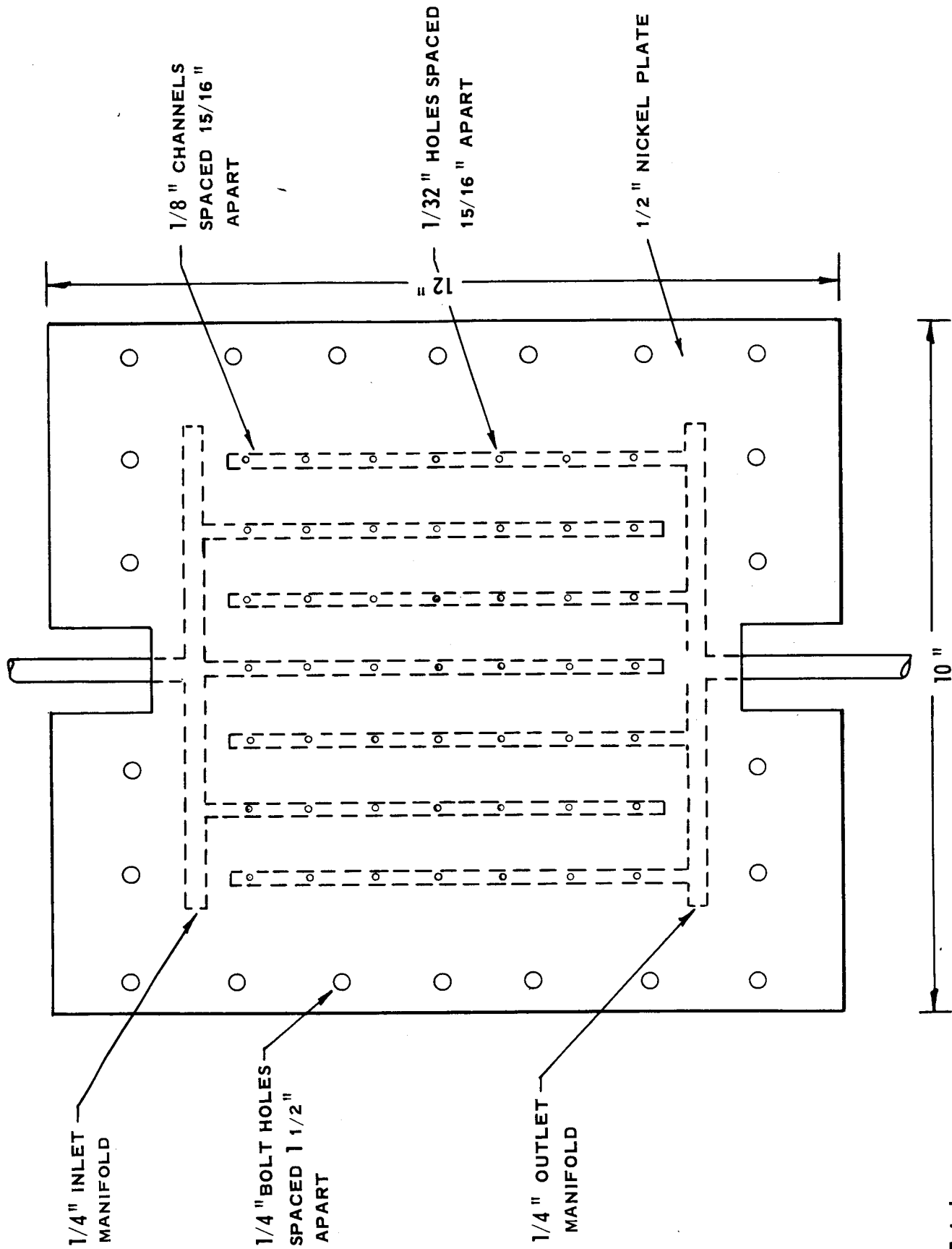
These data show that performance losses during life-testing at 125°C occur on both sides of the cell, and to a greater extent on the hydrogen side. The differences between the "gas side" and "matrix side" polarization curves indicate that life test performance losses may be due to an increasing occlusion of asbestos in the electrode pores. Therefore, it is not yet certain whether there is any actual loss of catalytic activity at 125°C.

4. LARGE CELL FABRICATION

At present a flat plate 6" x 6" active area cell is being used for large cell testing. The cell has been described previously in detail⁽²⁾. The gas distribution system of each face plate is shown in Figure 4-1. Gas enters and leaves the active area via holes distributed evenly along alternate parallel channels. The cell is sealed by gaskets made of either PTFE or PTFE-taped silicone rubber. The cell has operated satisfactorily at atmospheric pressure. Pressure tests showed that the cell can hold, initially at least, 60 psig of hydrogen at temperatures up to 200°C without gas leakage. However, the suitability of the gaskets after long periods of compression at 150-200°C is an unknown factor.

A 6" x 6" active area cell was designed for large cell life-testing at pressures up to 60 psig. The design is shown in detail in Figure 4-2. The gas distribution system is identical to that of the flat plate cell. Sealing of electrolyte and gas is provided by interlocking lands and grooves, which compress the outer portion of the matrix, and by a PTFE "O" ring. This method of sealing has proven to be satisfactory in the 2" x 2" cell used for life-testing at pressures, thus far, up to 15 psig. Fabrication was scheduled for three cells of this design.

6" X 6" CELL: FLAT PLATE DESIGN



6" x 6" CELL: LAND AND GROOVE DESIGN

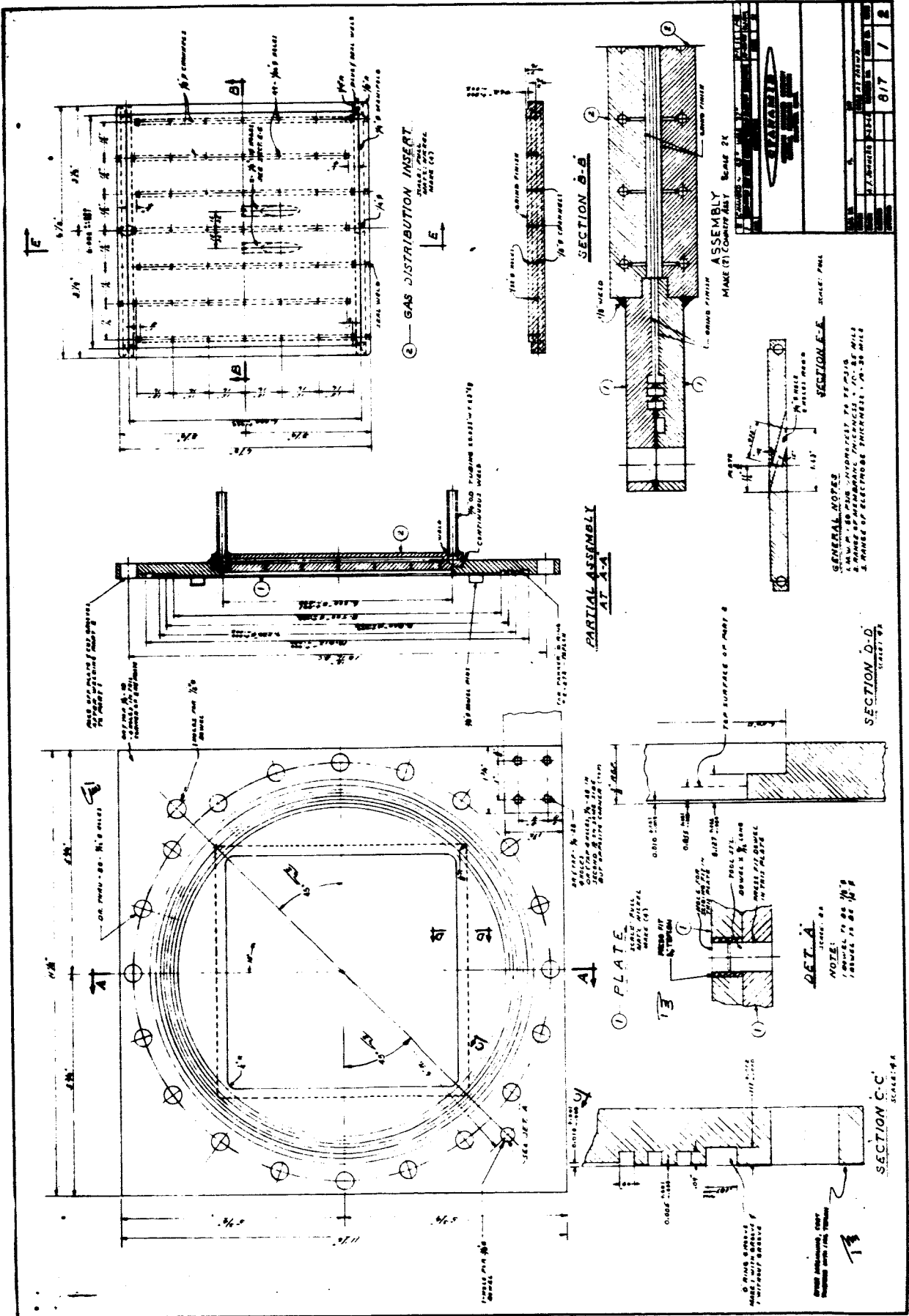


FIGURE 4-2

5. LARGE CELL TESTING

The effect of scale-up on initial performance was studied in the 6" x 6" cell. Two life-tests were also run. The active area of this cell is 45 times that of the 1" cells used for the investigation of operating variables and 9 times that of the cells used for small cell life testing. Runs were made with AB-40 electrodes and a 20 mil ACCO-I Asbestos matrix at 100°C, 50% KOH and 0 psig. The electrodes were pre-wet with KOH solution.

5.1 Initial Performance

Table 5-1 compares the initial performance of three different runs in the 6" x 6" cell with that of a one inch cell using the same electrodes. All runs in the six-inch cells with pre-wet electrodes exhibited the performance boost between the first and second polarization curves generally obtained with dry electrodes in one-inch cells. Both the first and second polarization voltages scaled up within 0-20 mv at current densities up to at least 600 ma/cm².

The resistance in the one-inch cell was 21 milliohms. For a 45-fold scale-up in active area, the resistance of the 6" x 6" cell should be 0.47 milliohms. The measured resistance was 0.64-0.96 milliohms. It is not yet clear whether these are true resistance values particularly since the initial performance scaled-up so closely.

5.2 Life Tests

In the 6" x 6" cell life tests, removal of product water simulated that in a battery system operating with a recycle hydrogen stream and dead-ended oxygen. The inlet hydrogen was humidified by sparging through a thermostatted

TABLE 5-1

Initial Performance: 6" x 6" Cell

Electrodes: AB-40
 Matrix: 20 mil ACCO-I Asbestos
 Temperature: 100°C
 KOH Conc.: 50%
 Pressure: 0 psig

Run	Polarization Curve	Cell Resistance (Milliohms)	Working Voltage at Current Density (ma/cm ²) of:									
			0	100	200	300	400	500	600	800	1000	
7556-3	1	.94	1.16	.93	.89	.85	.85	.85	.78	.75	.71	.62
	2	.96	-	.94	.90	.87	.84	.80	-	-	.73	.63
	3	.96	-	-	-	-	-	-	-	-	-	-
7556-8	1	.70	1.07	.95	.91	.87	.83	.83	.79	.74	.64	.57
	2	.65	-	-	-	-	-	-	-	-	-	-
7556-23	1	.74	1.10	.93	.89	.86	.82	.82	.79	.74	.63	.52
	2	.83	-	-	-	-	-	-	-	-	-	-
1" Cell	1	.21	1.17	.93	.89	.86	.83	.83	.79	.76	.68	.61
	2	.21	1.08	.96	.92	.89	.86	.86	.83	.80	.73	.63

water saturator. The inlet oxygen was dry and, while not actually dead-ended, removed only 2-3% of the product water. Testing was aimed first at determining whether serious voltage decline rates (> 6 mv/100 hours) are encountered at current densities in the range 100-400 ma/cm². Life test results are shown in Table 5-2.

Life test 7556-8 was run at 100 ma/cm². The inlet hydrogen was humidified at 44°C. The voltage of the second polarization curve (0.976 v) fell within three hours to that of the first polarization curve (0.951 v) and then was nearly constant during the next 65 hours. The run was terminated by a sudden overnight failure resulting apparently from rupture of the matrix by the compression of the inner edges of the gasket.

To prevent matrix rupture, life test 7556-23 employed a frame of thin PTFE sheet around the matrix, an arrangement used previously in small cell life testing. The time history of this test is shown in Figure 5-1. The test was started on dry gases. After 24 hours the inlet hydrogen stream was humidified at 44°C with the exit flow rates set to maintain 50% KOH at 100°C. At 100 ma/cm², the voltage of the second polarization curve (0.965 v) fell during three hours to 0.949 v and then declined at an acceptable rate (3.6 mv/100 hrs.) for 200 hours. At 200 ma/cm² the initial voltage was 0.897 v and the decline rate during 100 hours (3.0 mv/100 hrs.) was also acceptable.

At 300 ma/cm², the initial voltage was 0.851 v. During 190 hours the decline rate was high (7.5 mv/100 hours). Attempts were made to obtain more stable operation by increasing the humidity of the inlet hydrogen, while maintaining an average of 50% KOH in the cell through increased flow rate. In principle this should decrease the maximum KOH concentration at any local point on the hydrogen electrode and thus tend

TABLE 5-2

Life Tests: 6" x 6" Cells

Run	Current Density (ma/cm ²)	Inlet Flow Ratio (H ₂ /O ₂)	Inlet Gas Condition		Total Elapsed Time (Hours)	Time at Given Condition (Hours)	Working Voltage		Overall Voltage Decline Rate (mv/100 hrs.)	Cell Resistance (Milliohms)		
			H ₂	O ₂			Initial	Maximum		Final	Initial	Minimum
7556-8	100	8	Humidified at 44°C	Dry	70	70	.951 (a)	.951	3.1	.69	.59	.61
7556-23	100	"	Humidified at 44°C	Dry	190	190	.949 (b)	.949	3.6	.66	.66	.72
	200	"	"	"	293	103	.897	.897	3.0	.72	.72	.72
	300	8-11	Humidified at 44-55°C	"	870 (c) 1113 (d)	577 243	.851	.851	10 (c)	.72	.72	.74 (c) .60 (d)

(a) Voltage declined rapidly to .951 from .976

(b) Voltage declined rapidly to .949 from .965

(c) Before first reversal of polarity

(d) After second reversal of polarity

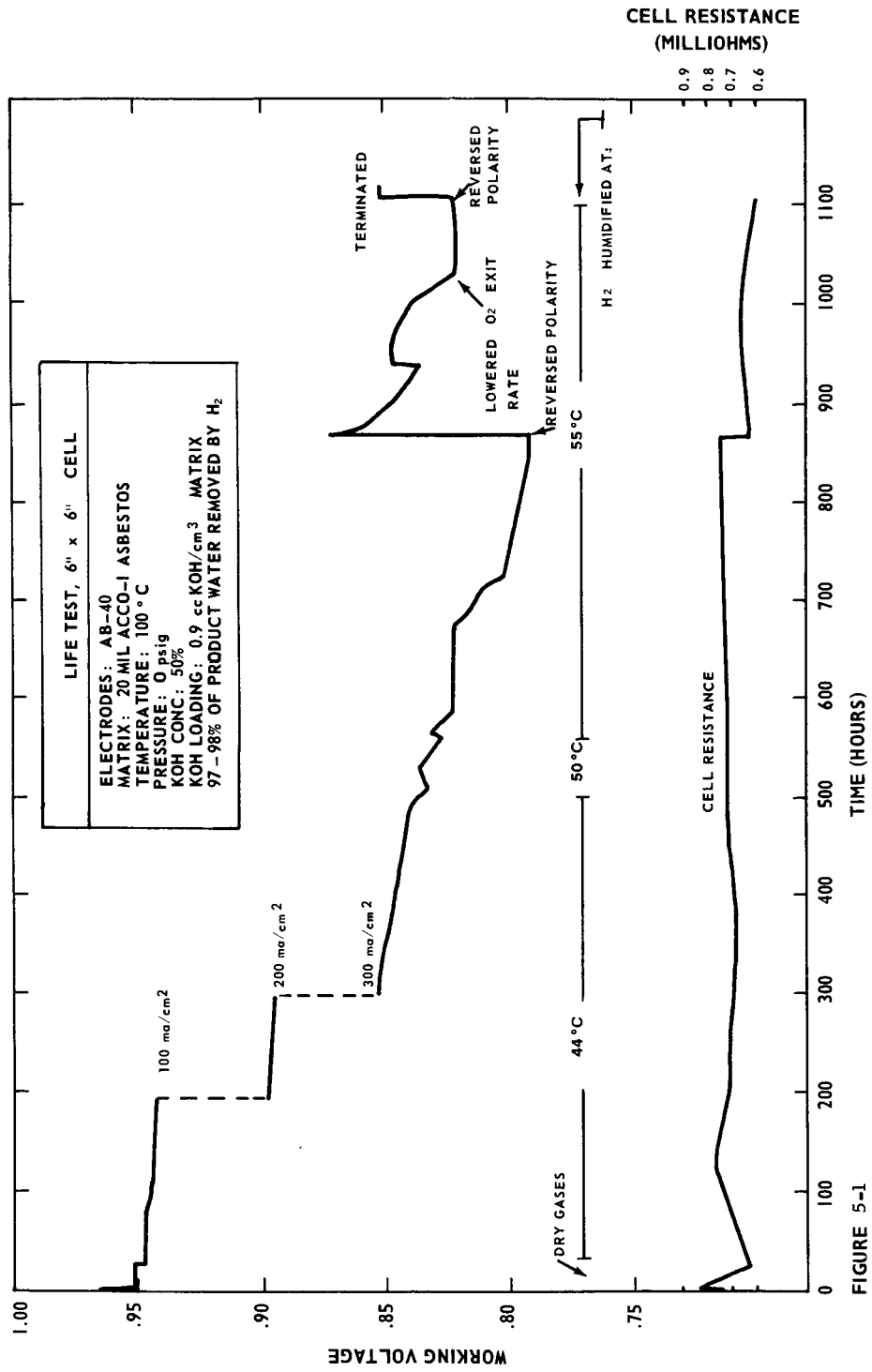


FIGURE 5-1

to prevent local solidification of KOH in the electrode pores. Accordingly, the humidifier temperature was raised from 44°C to 50°C for 48 hours, and then to 55°C. At these temperatures the partial pressures of water in the inlet hydrogen correspond to maximum KOH concentrations of 61%, 58% and 55% respectively (or 4%, 7% and 10% below the solubility limit at 100°C). At 50°C in the humidifier the voltage decline rate was 8 mv/100 hrs. However, for a period of 72 hours the voltage was constant at 0.821v. No comparable period of stable operation occurred while the hydrogen was humidified at 44°C.

For 577 hours at 300 ma/cm², the overall voltage decline rate was 10 mv/100 hrs. During this period there was no significant rise in cell resistance. The polarity of the cell was then reversed. The voltage rose immediately by 83 mv from 0.790v to 0.873v which was above the initial voltage (0.851v). Cell resistance decreased slightly from 0.74 to 0.62 ohms. The voltage then declined during 243 hours at an overall rate of 18 mv/100 hrs with no significant change in resistance.

An additional attempt was made to obtain stable performance by lowering the oxygen exit rate. Even at the very low oxygen exit rate employed throughout the run (45 cc/min) there may have been a tendency at 300 ma/cm² to dry out the oxygen side. No voltage loss occurred during the next 85 hours. This suggests that more stable performance might be achieved by humidifying or by actually dead-ending the oxygen stream.

A second reversal in polarity at 1113 hours restored the initial voltage (0.851v). The major gas stream, hydrogen, was then impinging on the same electrode and at the same points as it had during the first 880 hours of test. Restoration of the initial voltage suggests that no severe erosion occurred as a result of the high rates of flow (2500-3500 cc/min) used at 300 ma/cm². The run was terminated to permit a new run at 300 ma/cm², starting with a humidifier temperature of 55°C and a minimal oxygen exit rate.

Examination of the electrodes confirmed that erosion of the electrodes was insignificant. Approximately 20% of the inlet gas ports on each plate were found to be plugged with KOH, however, and this may have contributed to the overall decline observed.

6. FUTURE WORK

Work for the next quarter is planned for the following Tasks.

1. Investigation of Operating Variables

The empirical performance model will be completed. At preferred conditions of temperature, pressure and KOH concentrations, the effects of the fraction of product water removal at each electrode and of the humidity of the inlet gases on initial performance will be determined.

2. Materials Investigation

Evaluation of matrix materials for operation at 150-200°C will continue with ceria-P_TFE and thoria-P_TFE matrices.

3. Small Cell Life Testing

Life tests will be conducted at preferred operating conditions and current densities up to 1000 ma/cm² with the aim of obtaining stable operation for 1200 hours. Asbestos matrices will be used in these tests. Additional life tests will be run with promising matrices at 150-200°C.

4. Large Cell Testing

Life testing will be conducted at preferred operating conditions and current densities up to 300 ma/cm² with the aim of obtaining stable operation for 1000 hours. Asbestos matrices will be used in these tests.

7. REFERENCES

- (1) "Research and Development of High Performance Light Weight Fuel Cell Electrodes," American Cyanamid Company, Final Report, November 1, 1963, to October 31, 1964, NASA CR-54436.
- (2) "Development of High Performance Light Weight Electrodes for Hydrogen-Oxygen Fuel Cells," American Cyanamid Company, First Quarterly Report, April 5, 1965, to July 5, 1965, NASA CR-54759.
- (3) H. Lux, E. Renauer, and E. Betz, Z. anorg. u. allgem. Chem. 310, 305, (1961).
- (4) A. M. Adams, F. T. Brown and R. G. H. Watson in "Fuel Cells" (W. Mitchell, Jr. ed.) Chap. 4, (Interscience) 1963.
- (5) S. O. Pickering, J. Chem. Soc., 63, 890, (1893).
- (6) J. E. Clifford, and C. L. Faust, Research on the Electrolysis of Water with a Hydrogen-Diffusion Cathode to be Used in a Rotating Cell, Battelle Memorial Inst., Final Report June 1, 1961 to May 31, 1962, (Contract AF 33 (616) 8431, Project 6373) (AMRL TDR 62-94).

Revised 5/26/65

QUARTERLY DISTRIBUTION LIST

One copy is to be sent to each addressee, unless otherwise indicated.
Note that more than one addressee may be shown for the same address.

National Aeronautics & Space Administration
Washington, D.C. 20546
Attention: Ernst M. Cohn, Code RNW
George F. Eesenwein, Code MAT
J. R. Miles, Code SL
A. M. Andrus, Code ST

National Aeronautics & Space Administration
Scientific and Technical Information Facility
P.O. Box 5700
Bethesda, Maryland 20014 (2 copies + 1 reproducible)

National Aeronautics & Space Administration
Goddard Space Flight Center
Greenbelt, Maryland 20771
Attention: Thomas Hennigan, Code 632.2

National Aeronautics & Space Administration
Langley Research Center
Langley Station
Hampton, Virginia 23365
Attention: S. T. Peterson

National Aeronautics & Space Administration
Lewis Research Center
21000 Brookpark Road
Cleveland, Ohio 44135
Attn: B. Lubarsky, Mail Stop 500-201
R. L. Cummings, Mail Stop 500-201
H. J. Schwartz, Mail Stop 500-201
J. E. Dilley, Mail Stop 500-309
N. D. Sanders, Mail Stop 302-1
M. J. Saari, Mail Stop 500-202
R. R. Miller, Mail Stop 500-202
Technology Utilization Office, Mail Stop 3-16
(Project Manager), Solar & Chemical Power Branch
Mail Stop 500-201
(1 copy + 1 reproducible)
Library, Mail Stop 3-7
Report Control, Mail Stop 5-5

National Aeronautics & Space Administration
Marshall Space Flight Center
Huntsville, Alabama 35812
Attention: Philip Youngblood and R. Boehme

National Aeronautics & Space Administration
Ames Research Center
Moffett Field, California 94035
Mountain View
Attention: James R. Swain, Pioneer Project

National Aeronautics & Space Administration
Ames Research Center
Moffett Field, California 94035
Mountain View
Attention: Mr. T. Wydeven
Environmental Control Branch

National Aeronautics & Space Administration
Ames Research Center
Moffett Field, California 94035
Mountain View
Attention: Jon Rubenzer, Biosatellite Project

National Aeronautics & Space Administration
Manned Spacecraft Center
Houston, Texas 77058
Attention: Richard Ferguson (EP-5)
Robert Cohen, Gemini Project Office
F. E. Eastman (EE-4)

National Aeronautics & Space Administration
Western Operations Office
Santa Monica, California 90406
Attention: P. Pomerantz

Jet Propulsion Laboratory
4800 Oak Grove Drive
Pasadena, California 91103
Attention: Aiji Uchiyama

DEPARTMENT OF THE ARMY

U. S. Army Engineer R & D Labs.
Fort Belvoir, Virginia 22060
Attention: Dr. Galen Frysinger (Code SMOFB-EP)
Electrical Power Branch

U. S. Army Electronics R & D Labs.
Fort Monmouth, New Jersey
Attention: Arthur F. Daniel (Code SELRA/SL-PS)
David Linden (Code SELRA/SL-PS)

U.S. Army Electronics R & D Labs.
Fort Monmouth, New Jersey
Attention: Dr. Adolph Fischbach (Code SELRA/SL-PS)
Dr. H. F. Hunger (Code SELRA/SL-PS)

Research Office
R & D Directorate
Army Weapons Command
Rock Island, Illinois
Attn: Mr. G. Riensmith, Chief

U. S. Army Research Office
Chief, Rand D.
Department of the Army
3D442, The Pentagon
Washington, D. C. 20546
Attention: Dr. Sidney J. Mangram

U. S. Army Research Office
Physical Sciences Division
3045 Columbia Pike
Arlington, Virginia

Harry Diamond Labs.
Room 300, Building 92
Connecticut Avenue & Van Ness Street, N.W.
Washington, D. C.
Attention: Nathan Kaplan

Army Materiel Command
Research Division
AMCRD-RSCM T-7
Washington 25, D. C.
Attention: John W. Crellin

Natick Labs.
Clothing & Organic Materials Division
Natick, Massachusetts
Attention: Leo A. Spano

Natick Labs.
Clothing & Organic Materials Division
Natick, Massachusetts
Attention: Robert N. Walsh

U. S. Army Research Office
Box CM, Duke Station
Durham, North Carolina
Attention: Paul Greer

U. S. Army Research Office
Box CM, Duke Station
Durham, North Carolina
Attention: Dr. Wilhelm Jorgensen

U. S. Army Mobility Command
Research Division
Center Line, Michigan 48090
Attention: O. Renius (AMSMO-RR)

Hq., U. S. Army Materiel Command
Development Division
Washington 25, D. C.
Attention: Marshall D. Aiken (AMCRD-DE-MO-P)

DEPARTMENT OF THE NAVY

Office of Naval Research
Department of the Navy
Washington 25, D. C.
Attention: Dr. Ralph Roberts, Code 429
Head, Power Branch

Office of Naval Research
Department of the Navy
Washington 25, D. C.
Attention: H. W. Fox, Code 425

Bureau of Naval Weapons
Department of the Navy
Washington 25, D. C.
Attention: Milton Knight, Code RAAE-50

Bureau of Naval Weapons
Department of the Navy
Washington 25, D. C.
Attention: Whitwell T. Beatson, Code RAAE-52

U. S. Naval Research Laboratory
Washington, D. C. 20390
Attention: Dr. J. C. White, Code 6160

Bureau of Ships
Department of the Navy
Washington 25, D. C.
Attention: Bernard B. Rosenbaum, Code 340

Bureau of Ships
Department of the Navy
Washington 25, D. C.
Attention: C. F. Viglotti, Code 660

Naval Ordnance Laboratory
Department of the Navy
Corona, California
Attention: William C. Spindler (Code 441)

Naval Ordnance Laboratory
Department of the Navy
Silver Spring, Maryland
Attention: Philip B. Cole (Code WB)

DEPARTMENT OF THE AIR FORCE

Flight Vehicle Power Branch
Air Force Aero Propulsion Laboratory
Wright-Patterson Air Force Base, Ohio
Attention: J. E. Cooper (Code APIP)

Space Systems Division
Los Angeles Air Force Station
Los Angeles, California, 90045
Attention: SSSD

AF Cambridge Research Lab.
Attention: CRZE
L. C. Hanscom Field
Bedford, Massachusetts
Attention: Francis X. Doherty

AF Cambridge Research Lab.
Attention: CRZE
L. C. Hanscom Field
Bedford, Massachusetts
Attention: Edward Raskind (Wing F)

Rome Air Development Center, RSD
Griffiss AFB, New York 13442
Attention: Frank J. Mollura (RASSM)

ATOMIC ENERGY COMMISSION

Army Reactors, DRD
U. S. Atomic Energy Commission
Washington 25, D. C.
Attention: D. B. Hoatson

OTHER GOVERNMENT AGENCIES

Office, DDR&E: USW & BSS
The Pentagon
Washington 25, D. C.
Attention: G. B. Wareham

Staff Metallurgist
Office, Director of Metallurgy Research
Bureau of Mines
Interior Building
Washington, D. C. 20240
Attention: Kenneth S. Higbie

Institute for Defense Analyses
Research and Engineering Support Division
400 Army-Navy Drive
Arlington, Virginia 22202
Attention: Dr. George C. Szego

Institute for Defense Analyses
Research and Engineering Support Division
400 Army-Navy Drive
Arlington, Virginia 22202
Attention: R. Hamilton

Power Information Center
University of Pennsylvania
Moore School Building
200 South 33rd Street
Philadelphia 4, Pennsylvania

Office of Technical Services
Department of Commerce
Washington, D. C. 20009

PRIVATE INDUSTRY

Aeronutronic Division
Philco Corporation
Ford Road
Newport Beach, California 92663
Attention: Dr. S. W. Weller

Alfred University
Alfred, New York
Attention: Prof. T. J. Gray

Allis-Chalmers Mfg. Company
1100 South 70th Street
Milwaukee, Wisconsin 53201
Attention: Mr. John Plattner

Allison Division
General Motors Corporation
Indianapolis 6, Indiana
Attention: Dr. Robert B. Henderson

American Machine & Foundry
689 Hope Street
Springdale, Connecticut
Attention: Dr. L. H. Shaffer
Research & Development Division

Arthur D. Little, Inc.
Acorn Park
Cambridge, Mass., 02140
Attention: Dr. Ellery W. Stone

Astropower, Incorporated
Douglas Aircraft Company, Inc.
2121 College Drive
Newport Beach, California
Attention: Dr. Carl Berger

Atomics International, Division of
North American Aviation, Inc.
Canoga Park, California
Attention: Dr. H. L. Recht

Battelle Memorial Institute
505 King Avenue
Columbus, Ohio 43201
Attention: Dr. C. L. Faust

Bell Telephone Laboratories, Inc.
Murray Hill, New Jersey
Attention: Mr. U. B. Thomas

Clevite Corporation
Mechanical Research Division
540 East 105th Street
Cleveland, Ohio 44108
Attention: A. D. Schwope

Electrochimica Corporation
1140 O'Brien Drive
Menlo Park, California
Attention: Dr. Morris Eisenberg

Electro-Optical Systems, Inc.
300 North Halstead Street
Pasadena, California
Attention: E. Findl

Engelhard Industries, Inc.
497 DeLancy Street
Newark 5, New Jersey
Attention: Dr. J. G. Cohn

Esso Research & Engineering Company
Products Research Division
P. O. Box 121
Linden, New Jersey 07036
Attention: Dr. Robert Epperly

The Franklin Institute
Benjamin Franklin Avenue at 20th St.
Philadelphia 3, Pennsylvania
Attention: Robert Goodman

Garrett Corporation
1625 Eye Street, N. W.
Washington 6, D. C.
Attention: George R. Sheperd

General Electric Company
Direct Energy Conversion Operations
Lynn, Massachusetts
Attention: Dr. E. Oster

General Electric Company
Missile & Space Vehicle Department
P. O. Box 8555
Philadelphia, Pennsylvania 19101
Attention: E. W. Kipp, Room T-2513

General Electric Company
Research Laboratory
Schenectady, New York
Attention: Dr. H. Liebhafsky

General Motors Corporation
Box T
Santa Barbara, California
Attention: Dr. C. R. Russell

General Motors Corporation
Research Laboratories
Electrochemistry Department
12 Mile & Mound Roads
Warren, Michigan 48090
Attention: Mr. Seward Beacom

G. M. Defense Research Lab.
P. O. Box T
Santa Barbara, California
Attention: Dr. Smatko

Globe-Union, Inc.
900 East Keefe Avenue
Milwaukee, Wisconsin 53201
Attention: Dr. W. Towle

Hughes Research Laboratories Corp.
Malibu, California
Attention: T. M. Hahn

Institute of Gas Technology
State & 34th Streets
Chicago, Illinois
Attention: Mr. Bernard Baker

Ionics, Incorporated
152 Sixth Street
Cambridge, Massachusetts 02142
Attention: Dr. Werner Glass

John Hopkins University
Applied Physics Laboratory
8621 Georgia Avenue
Silver Spring, Maryland
Attention: W. A. Tynan

Leesona Moos Laboratories
Lake Success Park
Community Drive
Great Neck, New York
Attention: Dr. A. Moos

Midwest Research Institute
425 Volker Boulevard
Kansas City 10, Missouri
Attention: Dr. B. W. Beadle

Monsanto Research Corporation
Everett, Massachusetts 02149
Attention: Dr. J. Smith

North American Aviation Inc.
S&ID Division
Downey, California
Attention: Dr. James Nash

Power Sources Division
Whittaker Corporation
9601 Canoga Avenue
Chatsworth, California 91311
Attention: Dr. M. Shaw

Pratt & Whitney Aircraft Division
United Aircraft Corporation
East Hartford 8, Connecticut
Attention: Librarian

Radio Corporation of America
Astro Division
Heightstown, New Jersey
Attention: Dr. Seymour Winkler

Rocketdyne
6633 Canoga Avenue
Canoga Park, California
Attention: Library, Dept. 586-306

Space Technology Laboratories, Inc.
2400 E. El Segundo Boulevard
El Segundo, California
Attention: Dr. A. Krauz

Speer Carbon Company
Research & Development Laboratories
Packard Road at 47th Street
Niagara Falls, New York
Attention: Dr. L. M. Liggett

Stanford Research Institute
820 Mission Street
South Pasadena, California
Attention: Dr. Fritz Kalhammer

Texas Instruments, Inc.
13500 North Central Expressway
Dallas, Texas
Attention: Mr. Isaac Trachtenberg

Thiokol Chemical Corporation
Reaction Motors Division
Denville, New Jersey
Attention: Dr. D. J. Mann

Thompson Ramo Wooldridge, Inc.
23555 Euclid Avenue
Cleveland, Ohio 44117
Attention: Librarian

Tyco Laboratories, Inc.
Bear Hill
Waltham 54, Mass.
Attention: W. W. Burnett

University of Pennsylvania
Philadelphia, Pennsylvania 19104
Attention: Prof. John O'M. Bockris

University of Pennsylvania
Philadelphia, Pennsylvania 19104
Attention: Dr. Manfred Altman

Unified Science Associates, Inc.
826 South Arroyo Parkway
Pasadena, California
Attention: Dr. Sam Naiditch

Union Carbide Corporation
12900 Snow Road
Parma, Ohio
Attention: Dr. George E. Evans

University of California
Space Science Laboratory
Berkeley 4, California
Attention: Prof. Charles W. Tobias

Western Reserve University
Cleveland, Ohio
Attention: Prof. Ernest Yeager

Westinghouse Electric Corporation
Research and Development Center
Churchill Borough
Pittsburgh, Pennsylvania
Attention: Dr. A. Langer

Yardney Electric Corporation
40-50 Leonard Street
New York, New York
Attention: Dr. Paul Howard

The Western Company
Suite 802 RCA Building
Washington, D. C.
Attention: R. T. Fiske

Johns-Manville R & E Center
P. O. Box 159
Manville, New Jersey
Attention: Mr. J. S. Parkinson